Dynamics of two-dimensional melting

Annette Zippelius, B. I. Halperin, and David R. Nelson
Department of Physics, Harvard University, Cambridge, Massachusetts 02138
(Received 27 February 1980)

The dynamics of melting in two dimensions is studied, assuming that solids melt into liquids via a sequence of dislocation and disclination unbinding transitions. The hydrodynamics of solids, hexatics, and liquids in the presence of dislocations and disclinations is described as well as the dynamical response near the solid-hexatic and hexatic-liquid transitions. Although the theory is constructed with applications to free-standing liquid-crystal films in mind, it should be suitable with various modifications for films on solid substrates, lipid monolayers on water, and other systems.

I. INTRODUCTION

A. Purpose

There is now considerable theoretical and experimental interest in melting of thin films which are essentially two dimensional. Theoretically, one may be able to understand melting of these materials in terms of the dislocation mechanism proposed by Kosterlitz and Thouless.[1,2] According to this point of view, melting occurs when thermally activated dislocation pairs dissociate at sufficiently high temperatures.

Of course, dislocations have long been proposed as a mechanism for *three*-dimensional melting.[3] Indeed, it is very tempting to view ordinary melting in terms of a sudden proliferation of dislocation loops in the solid phase. Shockley[3] argued that a liquidlike viscosity would result from the response of a tangled array of dislocation lines to an applied stress. Unfortunately, little analytical progress has been made in elaborating this picture of a liquid as a "heavily dislocated solid."

The situation is quite different in two dimensions, where dislocations are pointlike imperfections. Recent theoretical analyses[4–6] have brought powerful tools developed in the renormalization-group theory of critical phenomena[7] to bear on this problem. In Ref. 5 (henceforth referred to as I), it was found that two separate phase transitions are required to complete the transition from solid to liquid in two dimensions. Dislocations unbind at a temperature T_m into a phase with short-range translational order, but with persistent correlations in the orientations of bond angles. The properties of this phase are similar to those of a nematic liquid crystal, except that triangular lattices melt into a phase with persistent *sixfold,* rather than *twofold* order. Paired disclinations in this hexatic liquid-crystalline phase ultimately unbind themselves, driving a second transition at a higher temperature T_i into an isotropic liquid.

A precise characterization of the three phases described above rests on the large distance behavior of translational- and orientational-order-parameter correlation functions. Translational order is described by the local Fourier components $\rho_{\vec{G}}(\vec{r})$ of the density evaluated at a set of reciprocal lattice vectors $\{\vec{G}\}$. For the theories we shall consider here, one can take

$$\rho_{\vec{G}}(\vec{r}) = e^{i\vec{G}\cdot\vec{u}(\vec{r})} , \tag{1.1}$$

where $\vec{u}(\vec{r})$ is the displacement field at position $\vec{r}$. Sixfold orientational order is characterized by the complex quantity

$$\psi(\vec{r}) = e^{6i\theta(\vec{r})} , \tag{1.2}$$

where $\theta(\vec{r})$ is the orientation relative to some fixed reference axis of the bond between two neighboring atoms (see Fig. 1). Two-dimensional solids are characterized by algebraic decay of translational correlations at large $\vec{r}$, but long-range order in the orientations,

$$\langle \rho_{\vec{G}}(\vec{r})\rho^*_{\vec{G}}(\vec{0})\rangle \sim r^{-\eta_G(T)} , \tag{1.3a}$$

$$\lim_{r\to\infty} \langle \psi(\vec{r})\psi^*(\vec{0})\rangle = \text{const} \neq 0 . \tag{1.3b}$$

It will be convenient to speak of "quasi-long-range

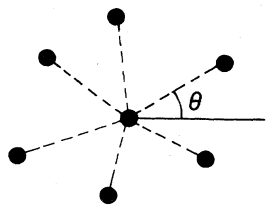

FIG. 1. "Bonds" (dashed lines) joining a central atom to its six nearest neighbors. Each such bond makes an angle θ with a fixed reference axis.

order" when correlations decay like power laws as in the Eq. (1.3a). Translational order decays exponentially in the hexatic phase, but there is quasi-long-range order in $\psi(\vec{r})$,

$$\langle \rho_{\vec{G}}(\vec{r})\rho^*_{\vec{G}}(\vec{0})\rangle \sim e^{-r/\xi_+(T)} , \tag{1.4a}$$

$$\langle \psi(\vec{r})\psi^*(\vec{0})\rangle \sim r^{-\eta_6(T)} . \tag{1.4b}$$

Both quantities exhibit short-range order in liquids,

$$\langle \rho_{\vec{G}}(\vec{r})\rho_{\vec{G}}(\vec{0})\rangle \sim e^{-r/\xi_+(T)} , \tag{1.5a}$$

$$\langle \psi(\vec{r})\psi^*(\vec{0})\rangle \sim e^{-r/\xi_\psi(T)} . \tag{1.5b}$$

A schematic and very tentative pressure-temperature phase diagram is shown in Fig. 2. All of the above phases appear, together with a vapor phase.

What makes two-dimensional melting particularly intriguing is the rich variety of experimental systems which can be investigated. As discussed in I, the theory is applicable with some modifications to physiadsorbed monolayers on a periodic substrate.[8] The Wigner crystal of electrons pinned to the surface of helium observed recently by Grimes and Adams[9] may also melt in a way consistent with the theory. Free-standing smectic liquid-crystal films[10,11] might provide some of the best realizations of isolated, two-dimensional liquid and solid phases. Birgeneau and Litster[12] have suggested that the theory could be helpful in understanding *bulk* smectic liquid-crystal phases. Finally, one might hope that the theory applies to lipid monolayers floating on water, provided transitions associated with the hydrocarbon chains can be excluded.

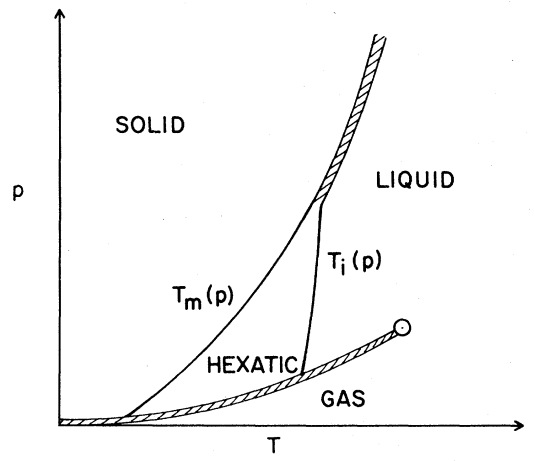

FIG. 2. Possible pressure-temperature phase diagram for circularly symmetric molecules with an attractive potential. Hatched lines indicate first-order transitions. The lines $T_m(p)$ and $T_i(p)$ are loci of the dislocation and disclination unbinding transitions discussed in the text. Many different phase diagrams are possible, and this figure represents only one guess.

To make contact with these experimental situations, it is particularly important to extend the equilibrium melting theory to dynamical situations. Indeed, many experiments actually measure the response of systems to space- and time-dependent external perturbations. Moreover, the predicted thermodynamic properties are not always particularly striking or even observable. Although there should be a jump discontinuity in the shear modulus and singular behavior in the structure factor at the dislocation unbinding transition, pressure-area isotherms and specific heat curves should have only unobservable essential singularities. As we shall see, the behavior of dynamical quantities can be more spectacular.

In this paper, we extend the melting theory to the time-dependent properties of solids, hexatics, and liquids, and study the dynamics of the transitions separating these phases. We shall focus in particular on situations where most of the conservation laws, applicable to truly two-dimensional matter, remain intact. Temperature fluctuations are neglected throughout, although this is not a fundamental limitation of the theory. Our results pertain most directly to free-standing smectic liquid-crystal films, where momentum and number density are conserved to a good approximation.

With suitable modifications, the theory can be taken over to other interesting experimental situations. For example, melting of a physiadsorbed monolayer on a glassy substrate could be treated by discarding the conservation of the momentum variable $\vec{g}(\vec{r},t)$ which enters most of our analysis. One must then introduce an extra term in the equation of motion for $\vec{g}$ which causes it to relax rapidly to a value determined by the local stress forces,

$$\frac{dg_i}{dt} = \partial_j \sigma_{ij} - \Gamma g_i . \tag{1.6}$$

Here, σ_{ij} is the usual stress tensor associated with a conserved momentum density and the term proportional to Γ breaks this conservation of $\vec{g}$. Conservation of number density must also be discarded, if the adsorbate is in equilibrium with a dense bulk vapor phase.

For lipids or other amphiphillic molecules floating on water,[13] one must solve simultaneously the hydrodynamic equations of the liquid substrate, together with those for the lipid monolayer phase, with suitable boundary conditions.[14] The transport coefficients worked out in this paper would enter as input parameters in such calculations. The dynamics of electrons on the surface of helium can be treated in a similar fashion, provided one takes account of effects associated with the long-range Coulomb interaction.

Some support for the equilibrium melting theory can already be found in recent computer experiments. Frenkel and McTague[15] find two distinct melting transitions, with no observable latent heat, in a molecular-dynamics simulation with a 6-12 Lennard-Jones potential. A computer simulation by Morf[16] suggests that the two-dimensional electron crystal observed by Grimes and Adams[9] melts at a temperature consistent with the theory, provided renormalization of the shear modulus is taken into account. The *dynamical* results reported here should also be testable by molecular-dynamics methods. The dynamical quantities measured by Frenkel and McTague are discussed in Sec. VI E. Our conclusions may be especially useful in estimating the times necessary to reach equilibrium in a computer experiment. There are pronounced "critical slowing down" effects (divergent relaxation times) near the dislocation and disclination unbinding transitions, so particular care is required in simulations near these temperatures. A pair of such temperatures, where equilibrium is reached very slowly, might lead to erroneous "hysteresis loops" in computer experiments.

B. Generalized hydrodynamics

Our treatment of melting dynamics consists of two parts. We first discuss the ordinary, defect-free hydrodynamics,[17] of the solid, hexatic, and liquid phases (Secs. II and III, below). This discussion focuses attention on a few long-wavelength, slowly varying modes determined by conservation laws, symmetry considerations, etc. One finds results parametrized by quantities like equilibrium elastic constants, and by a set of unknown transport coefficients.

In the remainder of the paper we concentrate on the dynamic behavior in the vicinity of the two transitions T_m and T_i. Our purpose is to predict the temperature dependence of the transport coefficients appearing in the hydrodynamic equations, and to analyze the breakdown of hydrodynamics at finite frequencies, near the transitions. The treatment here rests on a generalization of hydrodynamics to include an equilibrium concentration of defects. Specifically we regard the system near T_m as a solid with a small concentration of dislocations (bound dislocations for $T < T_m$; free dislocations and bound dislocations for $T > T_m$). Near T_i, we consider the system to be a hexatic together with a small concentration of disclinations. For simplicity we consider only the melting of a regular triangular solid.

The independent hydrodynamic equations in a particular system are associated with the appropriate conserved densities, as well as with the "phases" of any order parameters characterizing a locally broken continuous symmetry. In two-dimensional liquids, where there are no broken symmetries, four hydrodynamic equations describe conservation of the momentum $\vec{g}(\vec{r},t)$, number density $n(\vec{r},t)$, and energy density $\epsilon(\vec{r},t)$. At long wavelengths one finds a pair of longitudinal sound frequencies, as well as diffusive shear and thermal modes.

Hexatics are characterized by an additional term in the free energy, relative to that for a liquid, namely,

$$\delta F_H = \tfrac{1}{2} K_A(T) \int |\vec{\nabla}\Theta|^2 d^2r \quad . \tag{1.7}$$

Here, $\Theta(r)$ is related to a smoothed version of the microscopic bond-orientation order parameter (1.2),

$$\Psi(\vec{r}) = \langle \psi \rangle_{\text{cell}} \equiv |\Psi| e^{6i\Theta(\vec{r})} \quad , \tag{1.8}$$

where $\langle\ \rangle_{\text{cell}}$ means an average over a "cell" centered at $\vec{r}$. If there are no free disclinations present, it is always possible to find cells large enough so that $\Theta(\vec{r})$ is single valued and continuous. Cuts must, of course, be introduced to make the microscopic bond-angle field $\theta(\vec{r})$ single valued in the presence of disclinations. The Frank constant $K_A(T)$, which measures the energy associated with deformations in $\Theta(\vec{r})$, is related to $\eta_6(T)$ by[5]

$$\eta_6(T) = 18 k_B T/\pi K_A(T) \quad . \tag{1.9}$$

The temperature dependence of $K_A(T)$ between T_m and T_i was worked out in I, and is displayed in Fig. 3.

Five hydrodynamic modes emerge when an equation of motion for $\Theta(\vec{r},t)$ is coupled to the conserved densities. Longitudinal sound and thermal diffusion exist, just as in a liquid, but there are two transverse modes arising from the coupling of $\Theta(\vec{r},t)$ to the transverse momentum density. Just as in a nematic

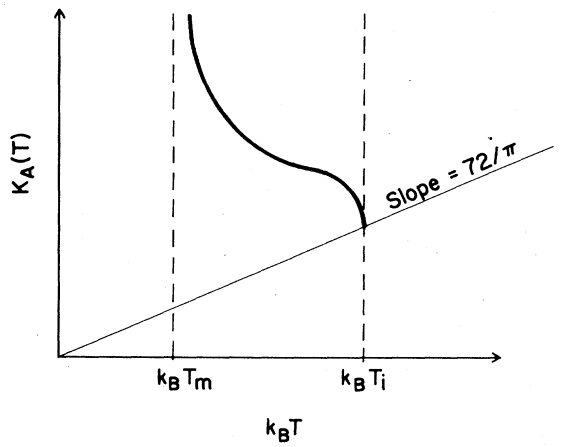

FIG. 3. Variation of the renormalized Frank constant $K_A(T)$ in the hexatic liquid-crystal phase. This quantity jumps discontinuously to zero at T_i and diverges like ξ_+^2 as $T \to T_m$. The jump discontinuity is preceeded by a square-root cusp, and must lie on a line with slope $72/\pi$.

liquid crystal,[18] the characteristic frequencies of these modes can be either purely diffusive, or else acquire a real part proportional to wave vector squared. Only two transport coefficients, in addition to the Frank constant $K_A(T)$, are necessary to completely characterize these excitations at long wavelengths. In Sec. VI E, we argue that these modes are purely diffusive near the transition temperature T_i found by Frenkel and McTague,[15] as well as near T_m.

In solids, the appropriate hydrodynamic order parameter is an average of (1.1),

$$\bar{\rho}_{\vec{G}}(\vec{r}) = \langle \rho_{\vec{G}} \rangle_{\text{cell}} \equiv |\bar{\rho}_G| e^{i\vec{G}\cdot\vec{U}(\vec{r})} \quad , \tag{1.10}$$

which defines a macroscopic displacement field $\vec{U}(\vec{r})$. For sufficiently large cell size, this field is single valued and continuous, provided dislocations exist only in neutral bound states. The two components of $\vec{U}(\vec{r})$, in addition to the conserved densities, must lead to six independent hydrodynamic variables in two-dimensional solids. As noticed by Martin *et al.*,[19] the shear and longitudinal sound waves (four modes in all), together with the thermal diffusion mode arising in standard treatments[20] of solid hydrodynamics, do not exhaust this number. They correctly identified the missing mode with a conserved "net defect density" $N_\Delta(\vec{r},t)$, defined as the difference between the density of interstitials N_i and the density of vacancies N_v,

$$N_\Delta(\vec{r},t) = N_i(\vec{r},t) - N_v(\vec{r},t) \quad . \tag{1.11}$$

The quantity $N_\Delta(\vec{r},t)$ is conserved, because vacancies and interstitials are created and destroyed in pairs in a solid, and fluctuations in N_Δ relax by a diffusive hydrodynamic mode.[19]

In Secs. II B and III C, where the results of Ref. 19 are rederived, we have found it convenient to eliminate $\delta n(\vec{r},t)$, the local change in the number density, in favor of $\delta N_\Delta(r,t)$,

$$\delta N_\Delta(\vec{r},t) = \delta n(\vec{r},t) + n_0 U_{ii}(\vec{r},t) \quad . \tag{1.12}$$

Here, n_0 is the average number density, and $\delta N_\Delta(\vec{r},t)$ is the local change in the net defect density. It is important to include in the free energy a term coupling δN_Δ to the lattice dilation U_{ii}, in addition to the usual elastic free energy,

$$F_{\text{el}} = \tfrac{1}{2}\int d^2r\,(2\mu_R U_{ij}^2 + \tilde{\lambda}_R U_{kk}^2) \quad , \tag{1.13}$$

where

$$U_{ij} = \tfrac{1}{2}(\partial_i U_j + \partial_j U_i) \quad , \tag{1.14}$$

and μ_R and $\tilde{\lambda}_R$ are elastic constants defined at constant net defect density.

Our discussion of hydrodynamics, and, indeed, all the analysis in this paper, neglects well-known problems[21] caused by the slow decay of time correlation functions in two dimensions. When "mode-coupling" nonlinearities in the hydrodynamic equations are taken into account, one typically finds divergences in the Kubo formulas for transport coefficients. The wave-vector- and frequency-dependent viscosity $\eta_R(k,\omega)$ of a liquid, for example, is expected to diverge for $k=0$ at low frequencies,

$$\eta_R(0,\omega) \sim \ln^{1/2}(1/\omega) \quad . \tag{1.15}$$

Analogous divergences have been found[22] in transport coefficients describing two-dimensional solids and hexatics. It is unlikely, however, that such logarithmically weak singularities have observable consequences at experimentally accessible wave vectors and frequencies. The theory described here predicts much stronger divergences in certain transport coefficients as a function of temperature near the dislocation and disclination unbinding transitions.

Just as in ordinary phase-transition problems,[23] hydrodynamics becomes inadequate near the continuous phase transitions separating solids, liquids, and hexatics. To determine the dynamical response and behavior of transport coefficients near T_m and T_i, we must generalize our dynamical equations to include effects of dislocations and disclinations.

Dislocations and disclinations clearly can have an important effect on the microscopic displacement and bond-orientation fields. A simple illustration is provided by a square lattice solid with uniform shear boundary conditions (Fig. 4). After a sufficiently long time, dislocation pairs should nucleate, unbind, and travel to the edges, relaxing the internal stresses[24] (Fig. 4). Although this kind of "plastic flow" can be treated using the diffusive model described in Sec. IV D, we shall focus here on similar effects produced by motion of *free* dislocations, regarding the hexatic phase as a kind of "heavily dislo-

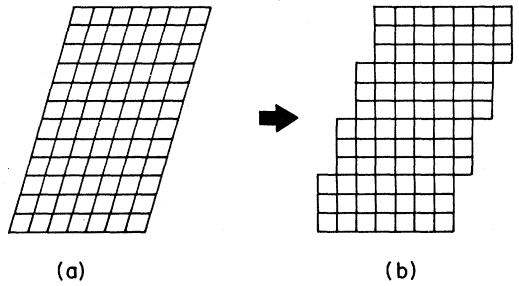

FIG. 4. Relaxation of a crystal under applied shear, by the motion of dislocations through the sample (plastic flow). Crystal (b) satisfies the same macroscopic boundary conditions as (a), but there are no internal stresses.

cated solid." We expect a density

$$n_f \approx \xi_+^{-2} \tag{1.16}$$

of screened free dislocations (with a screening length of order ξ_+) in the hexatic phase, where $\xi_+(T)$ is the correlation length defined by Eq. (1.4a). Near T_m it has a very strong temperature dependence,[5,6]

$$\xi_+(T) \sim \exp(b/|T - T_m|^{0.36963\cdots}) \ , \tag{1.17}$$

where b is a constant. If the recent theories of dislocation-mediated melting are correct, the combination of free dislocation motion and solid hydrodynamics should produce the characteristic excitations of a hexatic, with transport coefficients depending on n_f. At finite frequencies, *bound* dislocation pairs will also contribute to the dynamics, both above and below T_m.

Disclinations play a very similar role near T_i. Disclination motion couples to the microscopic bond orientation field in much the way that vortices affect two-dimensional superflow.[25,26] Regarding a liquid as a hexatic with a free disclination density

$$n_f^{(6)} \approx \xi_\psi^{-2} \ , \tag{1.18}$$

with[5]

$$\xi_\psi \approx \exp(b'/|T - T_i|^{1/2}) \ , \tag{1.19}$$

we can determine the temperature dependence of liquid transport coefficients just above T_i. Bound disclination pairs must be taken into account at finite frequencies.

To implement this program we have constructed "semimicroscopic" dynamical models of solids with dislocations and of hexatics with disclinations. In solids, we allow moving dislocations to interact with a microscopic strain field $u_{ij}(\vec{r},t)$ and a microscopic net defect density $\delta n_\Delta(\vec{r},t)$. The coupling to defects is important, since dislocations "climb" (move perpendicular to their Burgers vector) only in the presence of vacancies and interstitials.[24] Defects are not required for a dislocation to "glide" parallel to its Burgers vector. Disclinations interact with the *microscopic* bond-orientation field $\theta(\vec{r},t)$.

Our model equations resemble Maxwell's equations, in the way that dislocation and disclination charge densities and currents couple to the semimicroscopic hydrodynamic variables. Just as in the electrodynamics of metals and insulators, constitutive relations are used to eliminate dislocation and disclination currents, and obtain a closed set of equations. The form of the constitutive relations is determined by a temperature-dependent division of dislocations and disclinations into free and bound pairs. Bound singularities may be incorporated into a kind of "dielectric constant," while free singularities give rise to a "conductivity" proportional to their density.

C. Results and outline

The principal result of this paper is a semimicroscopic model of melting dynamics, which combines the correct conservation laws and symmetries with important dynamical effects due to dislocations and disclinations. The equations of motion defining the model can be applied to a wide variety of interesting experimental situations. Of course, the modifications necessary for systems on substrates described in Sec. I A must be made. Although applications to specific experiments have not been worked out in detail, there are a variety of interesting results, pertaining most directly to free-standing liquid-crystal films, which we summarize here.

Figure 5 shows different regions of the temperature–wave-vector plane, corresponding to different kinds of transverse excitations. Below T_m, one finds the usual shear sound waves, which propagate even *above* T_m at finite wavelengths. This behavior is consistent with a uniform shear modulus which drops abruptly to zero at T_m,[1,2,5] but is continuous and nonzero through T_m at finite wave vectors and frequencies. Damping caused by coupling of shear sound to dislocations increases until shear waves become ill defined in a region above T_m such that

$$q \approx \text{const}\, \xi_+^{-2} \ . \tag{1.20}$$

Below T_m, we expect that bound dislocation pairs contribute an anomalous damping to shear waves, which tends to zero at long wavelengths as a temperature-dependent power of the wave vector q. Although we have not studied this effect in detail, it is very similar to the anomalous damping of third sound worked out in Ref. 26.

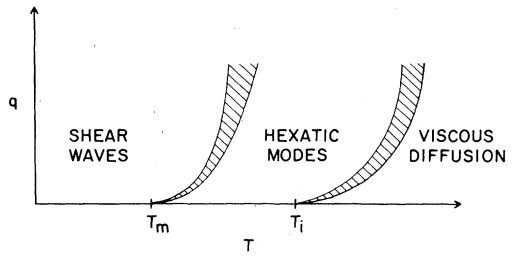

FIG. 5. Different regions of the wave-number–temperature plane describing different kinds of transverse excitations. Transverse sound propagates below T_m and above T_m up to the blurred region where $k \sim \text{const}\, \xi_+^{-2}$. In the hydrodynamic region $(k\xi_+) \ll 1$ above T_m one finds the two diffusive excitations of the hexatic phase, which exist also above T_i at finite wavelengths and change into liquidlike excitations for $k \lesssim \xi_\psi^{-1}$.

As q tends to zero at fixed $T > T_m$, one eventually passes through the region (1.20), and finds the characteristic excitations of a hexatic. Here, both hexatic frequencies are diffusive, with no real part,

$$\omega_+ \approx -D_+ q^2 i, \quad \omega_- \approx -D_- q^2 i \quad . \tag{1.21}$$

The diffusivity D_- remains finite for q very small as $T \to T_m^+$, while D_+ diverges strongly,

$$D_+ \sim \xi_+^2 \quad . \tag{1.22}$$

This behavior is only manifest for $q << \text{const}\, \xi_+^{-2}$, however, and may be difficult to observe experimentally. As one would expect intuitively, the viscosity of the hexatic phase is inversely proportional to the density of free dislocations, so that the viscosity diverges as ξ_+^2, when $T \to T_m^+$.

As shown in Fig. 2, the Frank constant $K_A(T)$ is expected to remain finite as T approaches the transition T_i to the isotropic phase. Correspondingly, one finds transverse hexatic hydrodynamic modes *above* T_i at finite wavelengths, with a changeover into liquidlike excitations for

$$q \approx \xi_\psi^{-1} \quad . \tag{1.23}$$

In the liquid hydrodynamic region ($q << \xi_\psi^{-1}$), the shear viscosity remains continuous through T_i, and becomes equal to the viscous coefficient $\eta(T)$ in the hexatic hydrodynamic equations,

$$\eta(T_i^+) = \eta(T_i^-) = \text{const} \quad . \tag{1.24}$$

There is actually some ambiguity in the definition of a hexatic shear viscosity, since there are *two* transverse diffusive modes. If, following Frenkel and McTague,[15] one defines an effective shear viscosity η_{eff} in terms of the zero-frequency transverse-momentum correlation function, the resulting quantity should jump discontinuously to a *larger* value as T is decreased through T_i. This jump is related to the jump in $K_A(T)$ at T_i, and will be rounded off at finite wave vectors and frequencies (see Fig. 3 of Ref. 15). The relation of the hexatic hydrodynamic parameters to various macroscopic measurements of an effective viscosity is discussed in Appendix A. Gradients in the bond-orientation field relax to zero more and more slowly as $T \to T_i^+$, at a rate proportional to ξ_ψ^{-2}.

Important insights into two-dimensional melting could be obtained by studying the response to a uniform, time-dependent shear near T_m. Such an experiment would be very analogous to the oscillating substrate experiment of Bishop and Reppy,[27] which showed clearly the importance of vortices in understanding superfluid helium films. It should be very straightforward to adapt the analysis of Ambegaokar *et al.*[26] for the superfluid, and predict the frequency-dependent shear modulus and absorption of energy near T_m. The necessary equations of motion, which include effects of free and bound dislocations, are contained in Sec. V. We expect a peak in the absorption above T_m, and a finite frequency shear modulus which is continuous through the dislocation unbinding transition.

The propagation of longitudinal sound near T_m is also quite interesting. Compressional sound waves propagate with characteristic frequencies,

$$\omega_l^{\pm} = \pm c_l q - \tfrac{1}{2} D_l q^2 i \quad , \tag{1.25}$$

above the dislocation unbinding transition. Below T_m there are additional, nonanalytic contributions to the damping, similar to those discussed above for shear waves. The damping constant D_l diverges as $T \to T_m^+$ in the hexatic hydrodynamic region,

$$D_l \sim \xi_+^2 \quad , \tag{1.26}$$

and is associated with a diverging viscosity. At the same time, a mode which becomes defect diffusion below T_m exhibits "critical slowing down," relaxing at a rate ξ_+^{-2}. When measurements of $D_l(T)$ are carried out at *finite* momenta, we expect a maximum at temperatures above T_m such that

$$q \approx A \exp(-B/|T - T_m|^{0.369\,63\cdots}) \quad , \tag{1.27}$$

where A and B are constants. The sound velocity $c_l(T)$ should rise smoothly with decreasing temperatures from its hexatic value to a larger value in the solid. For reasons explained in Sec. V, the response to a uniform, time-dependent compression at T_m is somewhat more complicated than the corresponding shear experiment. Nevertheless, we expect an anomalous absorption of energy just above T_m, and a rise in the frequency-dependent bulk modulus with decreasing temperatures.

The remainder of this paper is arranged as follows: In Secs. II and III, we describe the long-wavelength static and hydrodynamic properties of solids, hexatics, and liquids. The capital letters U_i, δN_Δ, and Θ are used to denote the displacement, defect density, and bond-orientation fields in these sections to emphasize that these are macroscopic, smoothed analogs of the corresponding microscopic fields, with no singularities due to dislocations and disclinations. A semimicroscopic model of a solid with dislocations is described in Sec. IV, where u_i and δn_Δ denote microscopic versions of the displacement and defect density fields. The model is solved near the dislocation unbinding temperature in Sec. V. A similar program is carried out for a hexatic with disclinations in Sec. VI, where θ denotes a microscopic bond field.

The relation between the hydrodynamic coefficients and various measurements of the viscosity in the hexatic phase is discussed in Appendix A. Some computational details of our study of the dynamics near T_m are given in Appendixes B and C.

II. EQUILIBRIUM PROPERTIES

In this section, we review the long-wavelength properties of liquids, hexatics, and solids in equilibrium. Although liquids and hexatics are quite easy to treat, care is necessary to properly incorporate defects like vacancies and interstitials into the description of a solid. Temperature fluctuations will be neglected for simplicity.

A. Liquids and hexatics in equilibrium

Following the usual methods of equilibrium statistical mechanics,[28] we expect that the probability of fluctuations in the momentum density, $\vec{g}(\vec{r})$, and in the number density, $n(\vec{r})$, are given by a free energy in the liquid phase of the form,

$$F_L = \frac{1}{2mn_0}\int d^2r\,|\vec{g}(\vec{r})|^2 + \frac{B}{2n_0^2}\int d^2r\,[\delta n(\vec{r})]^2 \ . \tag{2.1}$$

Here, $\delta n(r)$ is the deviation of the number density from its equilibrium value n_0, and the probability of a fluctuation is proportional to $\exp(-F_L/k_BT)$. The quantity m is the mass of the constituent particles, while the inverse isothermal bulk modulus or isothermal compressibility is just

$$B^{-1} = -\frac{1}{A}\left(\frac{\partial A}{\partial p}\right)_T \ , \tag{2.2}$$

where A is the area of the system, and p the two-dimensional pressure.

According to the results of I, a phase of matter can exist in two dimensions with residual sixfold order in bond-angle correlations, but with short-range translational order. Fluctuations in the average bond-angle field $\Theta(\vec{r})$ of this hexatic phase may then be described by a free energy,

$$F_H = F_L + \tfrac{1}{2}K_A\int d^2r\,(\vec{\nabla}\Theta)^2 \ , \tag{2.3}$$

where K_A measures the resistance to long-wavelength distortions of the bond-angle field. Since disclinations have already been averaged out in this description we can take $\Theta(\vec{r})$ to be a single-valued, continuous function. The stiffness parameter $K_A(T)$, which is analogous to a Frank constant in a nematic liquid crystal, is expected to have the temperature dependence shown in Fig. 3, as one goes from the solid transition temperature T_m to the transition to a liquid at T_i.[5]

B. Solids in equilibrium

To apply the general formulas of thermodynamics to solids, we must know the free energy as a function of the elastic degrees of freedom and the conserved densities. As was pointed out by Martin *et al.*,[19] it is important to distinguish between local lattice deformations and local changes in the number density. At any nonzero temperature interstitials and vacancies are present in finite concentrations, allowing for mass transport independent of deformations of the lattice.

We shall consider only small deviations from a state of thermal equilibrium at a temperature T_0 and a reference pressure p_0. Expanding the free energy F up to second order in small fluctuating quantities, and assuming a constant pressure p_0 at the boundaries, we find

$$\begin{aligned} F = {} & \frac{1}{2n_0m}\int d^2r\,|\vec{g}(\vec{r})|^2 \\ & + \tfrac{1}{2}\int d^2r\,[2\mu_R U_{ij}^2(\vec{r}) + \tilde{\lambda}_R U_{ii}^2(\vec{r})] \\ & + \frac{1}{2n_0^2\chi_R}\int d^2r\,[\delta N_\Delta(\vec{r})]^2 \\ & + \frac{\gamma_R}{n_0}\int d^2r\ U_{ii}(\vec{r})\delta N_\Delta(\vec{r}) \ , \end{aligned} \tag{2.4}$$

where χ_R and γ_R are phenomenological coefficients, and the remaining quantities have been defined above, in the Introduction and in Sec. II A. (Throughout this paper we use a summation convention on Latin indices, and we use the notation U_{ij}^2 to mean $U_{ij}U_{ij}$.)

The physical interpretations of the four terms on the right-hand side of (2.4) are as follows. The first term is simply the kinetic energy associated with the momentum density $\vec{g}$. The second term represents the elastic energy of a deformed isotropic body, as given by continuum elasticity theory,[20] and neglecting any changes in the net defect concentration N_Δ, defined as the difference between the density of interstitials and vacancies. The third term is the free energy change due to a change in the net defect concentration when the lattice constant is held fixed. Finally, the fourth term gives the coupling between fluctuations in the defect density and the strain field; it is the only possible bilinear coupling between the tensor U_{ij} and the scalar δN_Δ. Fluctuations in the local number density $n(\vec{r})$ are accounted for by changes in U_{ii} and δN_Δ, as mentioned in the Introduction, and discussed further in Sec. III C below.

The coupling between the elastic degrees of freedom and fluctuations in the local temperature has been neglected in (2.4). The strength of this coupling is determined by the relative difference $(C_p - C_v)/C_v$ of the specific heats at constant pressure and at constant volume. This quantity is usually small in solids. However, temperature fluctuations can be easily incorporated into (2.4) by an additional

term in the free energy[20]

$$F_T = \frac{1}{2}\frac{C_v}{T_0}\int d^2r\,[\delta T(\vec{r})]^2 + \alpha_1 \int d^2r\,\delta T(\vec{r})\,U_{ii}(\vec{r}) + \alpha_2 \int d^2r\,\delta T(\vec{r})\,\delta N_\Delta(\vec{r}) \quad . \tag{2.5}$$

Temperature fluctuations could be accounted for in the liquid and hexatic phases in an analogous fashion. Henceforth, we shall neglect temperature fluctuations in the solid phase.

We may note that at low temperatures, there will be an equilibrium density of vacancies and interstitials N_v^0 and N_i^0, proportional to Boltzmann factors,

$$N_v^0 \propto e^{-E_v/k_BT}, \quad N_i^0 \propto e^{-E_i/k_BT} \quad , \tag{2.6}$$

where E_v and E_i are the enthalpy changes associated with the creation of a vacancy or interstitial. By definition, we have

$$\delta N_\Delta(\vec{r}) \equiv N_\Delta(\vec{r}) - N_\Delta^0 \quad , \tag{2.7}$$

$$N_\Delta^0 = N_i^0 - N_v^0 \quad . \tag{2.8}$$

It is easy to show that at low temperatures, the susceptibility χ_R is proportional to $(N_v^0 + N_i^0)/k_BT$, which is very small for sufficiently small T.

It will be convenient below, to consider the response of the solid to a small change in stress applied to the boundary. For this purpose, one should add to the interior free energy (2.4) a boundary term,

$$F^{(\sigma)} = \oint dl\,\sigma_{ij}\left(\tfrac{1}{2}\hat{n}_i U_j + \tfrac{1}{2}\hat{n}_j U_i + n_0^{-1}\hat{n}_i\hat{n}_j\Sigma_\Delta\right) \quad , \tag{2.9}$$

where the integral is along the boundary of the system. Here, and throughout this paper, $\sigma_{ij}(\vec{r})$ is the *deviation* of the stress tensor from its equilibrium value at the reference pressure p_0. The quantity $\vec{U}(\vec{r})$ is the displacement at point $\vec{r}$, and $\hat{n}$ is a unit vector in the plane of the film and normal to the boundary of the sample; i.e.,

$$\hat{n}\,dl = -\hat{z} \times d\vec{l} \quad , \tag{2.10}$$

where $\hat{z}$ is the normal to the sample, and $d\vec{l}$ is tangent to its boundary. The quantity $\Sigma_\Delta(\vec{r})$ appearing in (2.9) is the net number of extra atoms per unit length accreted at the surface because of the flow of interstitials and vacancies to this boundary. Conservation of particle number implies

$$\frac{\partial \Sigma_\Delta}{\partial t} = \hat{n}\cdot\vec{J}_\Delta \quad , \tag{2.11}$$

at the surface and

$$\frac{\partial N_\Delta}{\partial t} = -\vec{\nabla}\cdot\vec{J}_\Delta \quad , \tag{2.12}$$

in the interior, where $\vec{J}_\Delta$ is a macroscopic defect current. Thus

$$\frac{\partial}{\partial t}\oint dl\,\Sigma_\Delta = -\int d^2r\frac{\partial N_\Delta}{\partial t} \tag{2.13}$$

or equivalently

$$\oint dl\,\Sigma_\Delta = -\int d^2r\,\delta N_\Delta \quad . \tag{2.14}$$

Let us now specialize to the situation where the stress at the boundary is caused by a uniform hydrostatic pressure so that

$$\sigma_{ij} = -\delta_{ij}\delta p \quad , \tag{2.15}$$

where $\delta p = p - p_0$. Since $\vec{U}$ is single valued in the solid phase (no dislocations are present at this level of description), we can use Green's theorem to write

$$\tfrac{1}{2}\oint(\hat{n}_i U_j + \hat{n}_j U_i)dl = \int d^2r\,U_{ij} \quad . \tag{2.16}$$

Using (2.14) and (2.16), we can now transform the boundary free energy $F^{(\sigma)}$ to an integral over the area of the film, $F^{(\sigma)}(\vec{U}, \Sigma_\Delta) = F^{(\sigma)}(U_{ij}, \delta N_\Delta)$, where

$$F^{(\sigma)} \equiv \delta p \int d^2r\,(U_{ii} - n_0^{-1}\delta N_\Delta) \quad . \tag{2.17}$$

We may note that the integral in (2.17) is just δA, the change in area of the system, relative to the equilibrium area at pressure p_0.

In equilibrium the free energy must be minimized with respect to small variations of U_{ij} and δN_Δ

$$\delta(F + \bar{F}^{(\sigma)})/\delta U_{ij} = 0 \quad , \tag{2.18}$$

$$\delta(F + \bar{F}^{(\sigma)})/\delta(\delta N_\Delta) = 0 \quad . \tag{2.19}$$

For the pure compressions under consideration, (2.18) reads

$$(\mu_R + \tilde{\lambda}_R)U_{ii} + \gamma_R\delta N_\Delta/n_0 = -\delta p \quad , \tag{2.20}$$

describing a mechanical equilibrium, which is reached in a relatively short time, comparable to the system size divided by the longitudinal sound velocity. For complete equilibrium, (2.19) must also hold,

$$\chi_R^{-1}\delta N_\Delta/n_0 + \gamma_R U_{ii} = \delta p \quad . \tag{2.21}$$

The characteristic time scale for this equilibrium to be reached, however, is given by the defect diffusion time, which in the long-wavelength limit is much longer than an inverse sound frequency.

Solving (2.20) and (2.21) for U_{ii} and δN_Δ as functions of δp, one can express the compressibility (i.e., the inverse bulk modulus),

$$B^{-1} \equiv -\frac{1}{A}\frac{\delta A}{\delta p} = -\frac{U_{ii}}{\delta p} + \frac{1}{n_0}\frac{\delta N_\Delta}{\delta p} \quad , \tag{2.22}$$

in terms of γ_R, χ_R and the elastic constants μ_R, $\tilde{\lambda}_R$:

$$B^{-1} = (\mu_R + \tilde{\lambda}_R - \gamma_R^2\chi_R)^{-1}[1 + (\mu_R + \tilde{\lambda}_R + 2\gamma_R)\chi_R] \quad . \tag{2.23}$$

If one were to measure the bulk modulus at times long compared to the elastic relaxation time but short compared to the defect diffusion time, the resulting equilibrium would be determined by (2.20) and the relation $\delta N_\Delta = 0$. The effective bulk modulus in this situation would be

$$B_{\rm eff}^{-1} = -\frac{U_{ii}}{\delta p} = 1/(\mu_R + \tilde{\lambda}_R) \ . \tag{2.24}$$

It should be emphasized that in situations where the strain is nonuniform, the components U_{xx}, U_{xy}, and U_{yy} cannot be regarded as three independent variables at each point. The condition that U_{ij} is derived from a single-valued displacement function $\vec{U}(\vec{r})$ imposes restrictions on the strain. It is convenient to express U_{ij} in terms of a nonsymmetrized derivative of the displacement field,

$$U_{ij} = \tfrac{1}{2}(W_{ij} + W_{ji}) \ , \tag{2.25}$$

$$W_{ij} \equiv \partial_i U_j \ . \tag{2.26}$$

Then W_{ij} obeys the condition

$$\epsilon_{ki}\partial_k W_{ij} = 0 \ , \tag{2.27}$$

where ϵ_{ij} is the antisymmetric unit tensor

$$\epsilon_{ij} = \begin{pmatrix} 0 & 1 \\ -1 & 0 \end{pmatrix} \ . \tag{2.28}$$

When a net density of dislocations is present, it is no longer possible to derive W_{ij} from a continuous and single-valued displacement field $\vec{U}(\vec{r})$, and Eq. (2.27) is no longer valid.

III. HYDRODYNAMICS

In this section we review conventional hydrodynamics for the solid, hexatic liquid crystal and fluid phases, following Refs. 19 and 29. One first has to isolate those degrees of freedom whose relaxation rates go to zero in the long-wavelength limit. In all three phases the conserved densities of momentum $\vec{g}$, energy ϵ, and number n of particles have to be considered

$$\partial_t n(\vec{r},t) = -(1/m)\,\vec{\nabla}\cdot\vec{g}(\vec{r},t) \ , \tag{3.1}$$

$$\partial_t g_i(\vec{r},t) = \partial_j \sigma_{ij}(\vec{r},t) \ , \tag{3.2}$$

$$\partial_t \epsilon(\vec{r},t) = -\vec{\nabla}\cdot\vec{j}_\epsilon(\vec{r},t) \ . \tag{3.3}$$

All quantities are averages over a hydrodynamic volume, small with respect to macroscopic scales and large compared to microscopic scales.

A. Liquid hydrodynamics

For an isotropic fluid the conserved densities are the only slow variables. Equations (3.1)–(3.3) have to be supplemented by constitutive relations for the stress tensor σ_{ij} and the energy density current $\vec{j}_\epsilon$.[30]

$$\sigma_{ij} = -p\,\delta_{ij} + \sigma_{ij}^{\rm Dis} \ , \tag{3.4}$$

$$\sigma_{ij}^{\rm Dis} = \frac{\eta}{mn_0}[\partial_i g_j + \partial_j g_i - (\vec{\nabla}\cdot\vec{g})\delta_{ij}] + \frac{\zeta}{mn_0}(\vec{\nabla}\cdot\vec{g})\delta_{ij} \ , \tag{3.5}$$

$$\vec{j}_\epsilon = (\epsilon_0 + p_0)\frac{\vec{g}}{mn_0} - \kappa_T\vec{\nabla}T \ . \tag{3.6}$$

The quantity κ_T denotes the thermal conductivity, η and ζ the shear and bulk viscosity, and ϵ_0 and p_0 the equilibrium energy density and pressure. The arguments $(\vec{r},t)$ of all fluctuating quantities have been suppressed. Solving (3.1)–(3.6) in the long-wavelength limit, one finds in two dimensions propagating sound ($\omega_l^\pm$), one heat diffusion mode (ω_T), and a decoupled diffusion mode of the transverse momentum (ω_t). The eigenfrequencies are

$$\omega_l^\pm = \pm c_l k - \tfrac{1}{2} i D_l k^2 \ , \tag{3.7}$$

with

$$c_l^2 = B/mn_0 \tag{3.8}$$

and

$$D_l = \frac{\eta+\zeta}{mn_0} + \frac{\kappa_T}{mn_0 C_p}\left(\frac{C_p}{C_v} - 1\right) \ , \tag{3.9}$$

$$\omega_T = -i(\kappa_T/mn_0 C_p)k^2 \ , \tag{3.10}$$

and

$$\omega_t = -i(\eta/mn_0)k^2 \ . \tag{3.11}$$

If the coupling between temperature fluctuations and sound modes is neglected, the speed of sound is changed from its adiabatic value c_l to the isothermal value and the sound-wave damping has only a viscous contribution.

B. Hexatic hydrodynamics

Both the static and dynamical properties of the hexatic phase resemble those of nematic liquid crystals. Because of the underlying sixfold symmetry, fewer hydrodynamic parameters are required to characterize the motion than for a nematic.[17,18,31] There are five hydrodynamic modes in all, associated with number, energy, and momentum conservation, as well as the local orientational order. With the neglect of temperature fluctuations, we are left with four independent hydrodynamic equations.

Hydrodynamic equations of motion for $\Theta(\vec{r},t)$, $\vec{g}(\vec{r},t)$, and $n(\vec{r},t)$ which relax to an equilibrium probability distribution controlled by Eq. (2.3) are readily constructed using, say, the methods of Ref. 17. To linear order in these quantities, we find

$$\frac{\partial \delta n}{\partial t} = -\frac{1}{m}\vec{\nabla}\cdot\vec{g} \ , \tag{3.12}$$

$$\frac{\partial \vec{g}}{\partial t} = -\tfrac{1}{2}K_A(\hat{z}\times\vec{\nabla})\nabla^2\Theta - \frac{B}{n_0}\vec{\nabla}\delta n + \frac{\eta}{mn_0}\nabla^2\vec{g} + \frac{\zeta}{mn_0}\vec{\nabla}(\vec{\nabla}\cdot\vec{g}) \ , \tag{3.13}$$

$$\frac{\partial \Theta}{\partial t} = \frac{1}{2mn_0}\epsilon_{ij}\partial_i g_j + \kappa\nabla^2\Theta \ , \tag{3.14}$$

where η and ζ are shear and bulk viscosities, and $\hat{z}$ is a unit vector perpendicular to the plane of the hexatic. The irreversible coupling κ can be expressed as the product of a kinetic coefficient Γ_6 and the stiffness K_A,

$$\kappa = \Gamma_6 K_A \ . \tag{3.15}$$

The first term of (3.14) just gives the precession of bond angles in the local vorticity field (see Fig. 6). It has a counterpart in the first term of (3.13), which shows that the fluid moves in response to inhomogeneities in the bond-angle field. It is easy to check that, when appropriate Langevin noise sources are added to (3.12)–(3.14), the system relaxes to an equilibrium probability distribution given by $\exp(-F_H/k_BT)$. The terms coupling the bond angle and transverse momentum fields together can also be derived by considering the "Poisson-bracket" relation between Θ and $\vec{g}$.

Projecting Eqs. (3.12) and (3.13) onto the transverse and longitudinal parts of the momentum density $\vec{g}$, one finds the usual longitudinal sound excitations, with characteristic frequencies

$$\omega_l^{\pm}(q) = \pm c_l q - \tfrac{1}{2}D_l q^2 i \ , \tag{3.16}$$

where

$$c_l = (B/mn_0)^{1/2} \tag{3.17}$$

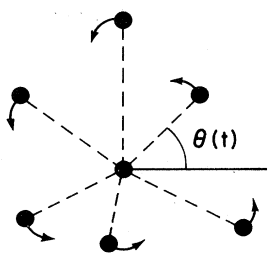

FIG. 6 Precession of the bond-angle field $\Theta(t)$ when $\vec{\nabla}\times\vec{g}\neq 0$.

and

$$D_l = (\eta+\zeta)/mn_0 \ . \tag{3.18}$$

If temperature fluctuations were considered, an adiabatic bulk modulus would replace the isothermal one, and there would be additional contributions to the damping.

The two transverse modes both involve the transverse momentum and the bond orientation as in nematic liquid crystals,[31,32] the eigenfrequencies can either be purely diffusive, or else acquire a propagating part proportional to q^2, depending on the sign of the quantity

$$\Delta = \frac{K_A}{mn_0} - \left(\frac{\eta}{mn_0}-\kappa\right)^2 \ . \tag{3.19}$$

For Δ negative, the modes are

$$\omega_t^{\pm}(q) = -\tfrac{1}{2}D_{\pm}q^2 i \ , \tag{3.20}$$

with

$$D_{\pm} = \frac{\eta}{mn_0}+\kappa \pm \left[\left(\frac{\eta}{mn_0}-\kappa\right)^2 - \frac{K_A}{mn_0}\right]^{1/2} \ , \tag{3.21}$$

while for positive Δ, they become

$$\omega_t^{\pm}(q) = \pm\tfrac{1}{2}\tilde{c}_t q^2 - \tfrac{1}{2}D_t q^2 i \ , \tag{3.22}$$

where

$$\tilde{c}_t = \left[\frac{K_A}{mn_0} - \left(\frac{\eta}{mn_0}-\kappa\right)^2\right]^{1/2} \tag{3.23}$$

and

$$D_t = \frac{\eta}{mn_0}+\kappa \ . \tag{3.24}$$

C. Solid hydrodynamics

In the solid phase we must incorporate the two components of the displacement field into our hydrodynamic description. These quantities relax slowly, even though there is no genuine long-range translational order in two dimensions. The bond-angle field, $\Theta(\vec{r},t)$ is not an independent hydrodynamic variable in this phase, but is, in fact, slaved to the displacement field $\vec{U}(\vec{r},t)$,

$$\Theta = \tfrac{1}{2}(\partial_x U_y - \partial_y U_x) \ . \tag{3.25}$$

In a perfect lattice the time derivative $mn_0\partial_t\vec{U}$ would be identical to the momentum density $\vec{g}$, implying $\delta n = -n_0 \mathrm{div}\vec{U}$. If, however, vacancies and interstitials are present, the number density differs from that of an ideal lattice by a "net defect density,"[19] defined to be the density of interstitials minus the

density of vacancies. With this definition, we have

$$\delta n(\vec{r},t) = -n_0 U_{ii}(\vec{r},t) + \delta N_\Delta(\vec{r},t) \ . \tag{3.26}$$

It follows from (3.1), (2.25), and (2.26) that the net defect density $N_\Delta(\vec{r},t)$ is conserved and obeys a continuity equation

$$\partial_t N_\Delta(\vec{r},t) = -\vec{\nabla}\cdot\vec{J}_\Delta(\vec{r},t) \ , \tag{3.27}$$

where $\vec{J}_\Delta(\vec{r},t)$ denotes a defect current, defined by

$$\vec{g}(\vec{r},t) = mn_0\partial_t\vec{U}(\vec{r},t) + m\vec{J}_\Delta(\vec{r},t) \ . \tag{3.28}$$

We have used the single valuedness of the displacement field in setting

$$\partial_t U_{ii} = \vec{\nabla}\cdot\partial_t\vec{U} \ . \tag{3.29}$$

To obtain a closed system of equations we must specify constitutive relations for $\vec{J}_\Delta$ and σ_{ij}. Neglecting the coupling to temperature fluctuations, σ_{ij} is given by

$$\sigma_{ij} = \sigma_{ij}^{\text{Rev}} + \sigma_{ij}^{\text{Dis}} \ , \tag{3.30}$$

with the same dissipative part as for an isotropic liquid (3.5) and

$$\sigma_{ij}^{\text{Rev}} = \frac{\delta F}{\delta U_{ij}} = 2\mu_R U_{ij} + \tilde{\lambda}_R U_{kk}\delta_{ij} + \gamma_R\frac{\delta N_\Delta}{n_0}\delta ij \ , \tag{3.31}$$

where μ_R and $\tilde{\lambda}_R$ are the isothermal elastic constants. For the defect density we assume purely relaxational dynamics

$$\vec{J}_\Delta = -\Gamma n_0^2\vec{\nabla}\frac{\delta F}{\delta(\delta N_\Delta)} = -\Gamma n_0\vec{\nabla}\left(\chi_R^{-1}\frac{\delta N_\Delta}{n_0} + \gamma_R U_{ii}\right) \ , \tag{3.32}$$

where Γ denotes a constant kinetic coefficient. At the boundary of the sample, the normal component of the defect current is given by

$$\vec{n}\cdot\vec{J}_\Delta = -n_0^2\Gamma^{(s)}\delta(F+F^{(\sigma)})/\delta\Sigma_\Delta = \Gamma^{(s)}n_0(\chi_R^{-1}\delta N_\Delta/n_0 + \gamma_R U_{ii} - \sigma_{ij}\hat{n}_i\hat{n}_j) \ , \tag{3.33}$$

where $\hat{n}$ is the unit vector normal to the boundary and $\Gamma^{(s)}$ is a boundary kinetic coefficient. The variational derivative in (3.33) is taken subject to the constraint that a change in Σ_Δ is accompanied by a change in N_Δ in the neighborhood of the boundary with $\oint\Sigma_\Delta\,dl = -\int\delta N_\Delta\,d^2r$. Clearly, the defect current to the surface should vanish when this derivative is zero.

These constitutive relations complete the hydrodynamic description of the solid phase. Altogether there are five slow modes (six, if temperature fluctuations are taken into account) with the equations of motion

$$\frac{\partial g_i}{\partial t} = \partial_j\left(2\mu_R U_{ij} + \tilde{\lambda}_R U_{kk}\delta_{ij} + \delta_{ij}\gamma_R\frac{\delta N_\Delta}{n_0}\right) + \frac{\eta}{mn_0}\partial_j[\partial_i g_j + \partial_j g_i - (\vec{\nabla}\cdot\vec{g})\delta_{ij}] + \frac{\zeta}{mn_0}\partial_i(\vec{\nabla}\cdot\vec{g}) \ , \tag{3.34}$$

$$\frac{\partial}{\partial t}\frac{\delta N_\Delta}{n_0} = \Gamma\nabla^2\left(\chi_R^{-1}\frac{\delta N_\Delta}{n_0} + \gamma_R U_{ii}\right) \ , \tag{3.35}$$

$$\frac{\partial U_i}{\partial t} = \frac{g_i}{mn_0} + \Gamma\partial_i\left(\chi_R^{-1}\frac{\delta N_\Delta}{n_0} + \gamma_R U_{jj}\right) \ . \tag{3.36}$$

The system (3.34)–(3.36) decouples into two transverse modes and three longitudinal ones. The transverse displacement can be recovered from the strain field $U_{ij}(\vec{k})$ by taking the projection

$$(k_n\epsilon_{ni}k_j/k^2)U_{ij}(\vec{k}) = \tfrac{1}{2}ik_n\epsilon_{ni}U_i(\vec{k}) \ . \tag{3.37}$$

Solving the coupled equations for the transverse momentum and displacement components, one finds the usual sound excitations with the dispersion relation,

$$\omega_t^{\pm} = \pm c_t k - ik^2\eta/2mn_0 \ , \tag{3.38a}$$

where

$$c_t^2 = \mu_R/mn_0 \ . \tag{3.38b}$$

The longitudinal modes involve coupled excitations of the defect density and the longitudinal components of momentum density and displacement field. The characteristic frequencies are

$$\omega_l^{\pm} = \pm c_l k - \tfrac{1}{2}ik^2 D_l \tag{3.39a}$$

with

$$c_l^2 = (2\mu_R + \tilde{\lambda}_R)/mn_0 \ , \tag{3.39b}$$

$$D_l = \frac{\eta+\zeta}{mn_0} + \Gamma\gamma_R + \Gamma\frac{\gamma_R^2}{2\mu_R+\tilde{\lambda}_R} \ , \tag{3.39c}$$

and

$$\omega_\Delta = -iD_\Delta k^2 \ , \tag{3.40a}$$

where

$$D_\Delta = \Gamma\chi_R^{-1} - \gamma_R^2\Gamma/(2\mu_R+\tilde{\lambda}_R) \sim \Gamma\chi_R^{-1} \ . \tag{3.40b}$$

For sufficiently small temperatures (small χ_R), longitudinal sound and defect diffusion decouple.

Note that the longitudinal sound velocity is given in terms of $2\mu_R + \tilde{\lambda}_R$, instead of the bulk modulus B discussed in Sec. II B. This result is certainly to be

expected, since defect diffusion times are slow compared to inverse longitudinal sound frequencies at long wavelengths. Indeed, the coupling of the defect density to longitudinal sound in a solid without temperature fluctuations is rather analogous to the coupling of thermal fluctuations to longitudinal sound in an ordinary liquid. In the latter situation, the sound velocity is usually given by an adiabatic rather than isothermal compressibility, since temperature fluctuations relax so slowly compared to sound propagation frequencies.

IV. MICROSCOPIC MODEL: A SOLID WITH DISLOCATIONS

Close to higher-order phase transitions, hydrodynamics must be generalized to include any additional strongly fluctuating variable responsible for the phase transition. In this section, we give a precise formulation of a model of a solid with dislocations, interacting with microscopic versions of the momentum, strain, and number-density fields described in Sec. III. As will become clear in the next two sections, the model reduces to the hydrodynamic description of either a solid or a hexatic at long wavelengths, depending on whether or not the dislocations are bound. Many microscopic models are possible; we describe here only the simplest one which gives the correct physics. In Sec. V, we shall use this model to determine the temperature dependence of various hydrodynamic parameters near T_m.

A. Microscopic fields in the presence of dislocations

When isolated dislocations are added to a solid phase, it is no longer possible to define a single-valued, continuous-displacement field $\vec{U}(\vec{r})$. If the dislocations are all bound in pairs (or other charge-neutral entities), however, one can define a continuous, single-valued displacement field by smoothing over regions of space large compared to the pair separations. Although dislocations will indeed be paired for solids in thermal equilibrium, we must construct equations of motion for microscopic strain and displacement fields in order to treat the transition into the hexatic phase, where dislocations are unbound.

Consider a set of M dislocations at a discrete set of points $\{\vec{R}^{(\nu)}\}$, $\nu = 1, 2, \ldots, M$, with Burgers vector $\vec{b}^{\nu}$. We may define a single-valued (but discontinuous) displacement field $\vec{u}(\vec{r})$, provided we introduce cuts K_ν, terminating at $\vec{R}^{(\nu)}$, such that $\vec{u}(\vec{r})$ jumps by $a_0\vec{b}^{(\nu)}$ upon crossing K_ν, in a direction counterclockwise with respect to rotations about $\vec{R}^{(\nu)}$. The quantity a_0 is the lattice constant of the triangular crystal, which we have introduced so that our Burgers vectors are dimensionless. The derivative of the displacement $w_{ij}(\vec{r})$ is then defined at all points *not* on a cut by

$$w_{ij}(\vec{r}) = \partial_i u_j(\vec{r}) \ , \tag{4.1}$$

in analogy to the macroscopic relation (2.6). At the cuts, we define $w_{ij}(\vec{r})$ as the limit of (4.1) as a cut is approached from either side, thus excluding a δ-function contribution. The same definition would arise if we took $w_{ij}(\vec{r})$ to be the derivative of a multivalued definition of the displacement field. Note that $w_{ij}(\vec{r})$ is single valued and continuous at all points $\vec{r}$ except the locations $\{\vec{R}^{(\nu)}\}$ of the dislocations themselves. If C is a contour enclosing $\vec{R}^{(\nu)}$, then we have

$$\oint_C w_{ij}\, dr_i = a_0 b_j^{(\nu)} \ . \tag{4.2}$$

It follows from (4.2) that

$$\epsilon_{kl}\partial_k w_{ij} = \Sigma_\nu b_j^{(\nu)} a_0 \delta(\vec{r} - \vec{R}^{(\nu)}) \tag{4.3}$$

so that the compatibility condition (2.27) is violated for these fields at isolated points.

A local, microscopic strain field $u_{ij}(\vec{r})$ can now be defined as

$$u_{ij} = \tfrac{1}{2}(w_{ij} + w_{ji}) \ , \tag{4.4}$$

and we can determine a local excess defect density $\delta n_\Delta(\vec{r})$ from

$$\delta n_\Delta(\vec{r}) \equiv \delta n(\vec{r}) + n_0 u_{ii}(\vec{r}) \equiv \delta n(\vec{r}) + n_0 w_{ii}(\vec{r}) \ , \tag{4.5}$$

where $\delta n(\vec{r})$ is the local fluctuation in number density.

We shall use the symbol $\vec{g}(\vec{r})$, as in the previous sections, to denote the local momentum density.

B. Microscopic free energy and equilibrium results

The microscopic fields defined above reduce to the macroscopic hydrodynamic fields of Secs. II and III in the absence of dislocations. We shall also assume a microscopic free energy analogous to (2.4), namely,

$$F_{\rm mic} = \tfrac{1}{2}\int d^2r\,(2\mu_0 u_{ij}^2 + \tilde{\lambda}_0 u_{kk}^2) + \frac{1}{2n_0 m}\int d^2r\,|\vec{g}|^2 + \frac{1}{2n_0^2}\chi_0^{-1}\int d^2r\,(\delta n_\Delta)^2 + \frac{\gamma_0}{n_0}\int d^2r\, u_{ii}\delta n_\Delta \ , \tag{4.6}$$

where the dislocation degrees of freedom enter through the constraint (4.3). Equation (4.6) then reduces to the hydrodynamic result (2.4), provided dislocations can be neglected. As will become apparent later, Eq. (4.6) also agrees with the results of continuum elastic theory when dislocations are present.[24]

The equilibrium properties associated with (4.6) were, in effect, worked out in I. To make contact with the results of I, we first integrate $\exp(-F_{\rm mic}/k_BT)$ over the defect number density δn_Δ and the momentum density g. The resulting elastic free energy F_E, with a constant term suppressed, is

$$F_E=\frac{1}{2}\int d^2r\,(2\mu_0 u_{ij}^2+\lambda_0 u_{kk}^2)\ , \tag{4.7}$$

where λ_0 is given by

$$\lambda_0=\tilde{\lambda}_0-\chi_0\gamma_0^2\ . \tag{4.8}$$

To understand the physical significance of λ_0, imagine a pressure force δp which acts to change the lattice constant, but does not couple directly to the mass density. Assume that there are no dislocations but that vacancies or interstitials are present. Equilibrium is then determined by an equation analogous to (2.20), but also by an equation analogous to (2.21) with the right-hand side set to zero. The resulting "elastic" bulk modulus then measures the Lamé coefficient λ_0.

$$B_{el}=\mu_0+\lambda_0\ . \tag{4.9}$$

The shear modulus is unaffected by the coupling to vacancies and interstitials. Dislocations renormalize μ_0, as well as $\tilde{\lambda}_0$, γ_0, and χ_0 in the combination (4.8).

To study this point further, one can decompose $u_{ij}(\vec{r})$ into a smoothly varying part $\phi_{ij}(\vec{r})$ and a part due to dislocations,

$$u_{ij}(\vec{r})=\phi_{ij}(\vec{r})+u_{ij}^{\rm dis}(\vec{r})\ . \tag{4.10}$$

The free energy F_E then breaks into two parts,

$$F_E=F_0+F_D\ , \tag{4.11}$$

with

$$F_0=\frac{1}{2}\int d^2r\,(2\mu_0\phi_{ij}^2+\lambda_0\phi_{kk}^2) \tag{4.12}$$

and where F_D is a vector Coulomb gas of interacting dislocations,

$$\frac{F_D}{k_BT}=\frac{-K_0}{8\pi}\sum_{\vec{r}\neq\vec{r}'}\left[\vec{b}(\vec{r})\cdot\vec{b}(\vec{r}')\ln\left(\frac{|\vec{r}-\vec{r}'|}{a}\right)-\frac{\vec{b}(\vec{r})\cdot(\vec{r}-\vec{r}')\vec{b}(\vec{r}')\cdot(\vec{r}-\vec{r}')}{|\vec{r}-\vec{r}'|^2}\right]+\frac{E_c}{k_BT}\sum_{\vec{r}}|\vec{b}(\vec{r})|^2\ . \tag{4.13}$$

The summations in (4.13) are over, say, a square lattice of possible sites for dislocations with lattice spacing equal to the core diameter a. The Burgers vector $\vec{b}(\vec{r})$ on site $\vec{r}$ may be written

$$\vec{b}(\vec{r})=m(\vec{r})\vec{e}_1+n(\vec{r})\vec{e}_2\ , \tag{4.14}$$

where $m(\vec{r})$ and $n(\vec{r})$ are integers (possibly zero) and $\vec{e}_1$ and $\vec{e}_2$ are unit vectors spanning the underlying triangular lattice. The coupling K_0 is

$$K_0=\frac{4\mu_0(\mu_0+\lambda_0)a_0^2}{(2\mu_0+\lambda_0)k_BT}\ , \tag{4.15}$$

while $E_c\equiv -k_BT\ln y_0$ is the core energy of a dislocation. When evaluating the partition sum associated with (4.13), one must sum over distinct complexions of Burgers vectors satisfying a charge neutrality condition,

$$\sum_{\vec{r}}\vec{b}(\vec{r})=0\ . \tag{4.16}$$

The elastic constants μ_0 and λ_0 are supposed to include effects due to excitations like vacancies, interstitials, and phonon anharmonicities, but not dislocations. To take dislocations into account, renormalization equations were constructed in Refs. 5 and 6, using a procedure which effectively increases the dislocation core radius from a to ae^l. A renormalized Coulomb-gas Hamiltonian results, with effective couplings $K(l)$ and $y(l)$, which are solutions of differential recursion relations,[5,6]

$$\frac{dK^{-1}}{dl}=\frac{3}{2}\pi y^2e^{K/8\pi}I_0\left(\frac{K}{8\pi}\right)-\frac{3}{4}\pi y^2e^{K/8\pi}I_1\left(\frac{K}{8\pi}\right)\ , \tag{4.17}$$

$$\frac{dy}{dl}=\left(2-\frac{K}{8\pi}\right)y+2\pi y^2e^{K/16\pi}I_0\left(\frac{K}{8\pi}\right)\ , \tag{4.18}$$

where $I_0(x)$ and $I_1(x)$ are modified Bessel functions. The solutions $K(l)$ and $y(l)$ must, of course, agree with K_0 and y_0 when $l=0$. For $K\leq 16\pi$ (above a temperature $T=T_m$), there is an instability toward large $y(l)$ signaling the dislocation unbinding transition predicted by Kosterlitz and Thouless.[1]

Two other results from the static theory will be of importance here. First, length-dependent elastic constants $\mu(l)$ and $\lambda(l)$ may be constructed, which are related to $K(l)$ in the same way that μ_0 and λ_0 are related to K_0, in Eq. (4.15). The recursion relations for $\mu(l)$ and $\lambda(l)$ are[5]

$$\frac{a_0^2}{k_BT}\frac{d\mu^{-1}}{dl}=3\pi y^2e^{K/8\pi}I_0\left(\frac{K}{8\pi}\right)\ , \tag{4.19}$$

$$\frac{a_0^2}{k_BT}\frac{d(\mu+\lambda)^{-1}}{dl}=3\pi y^2e^{K/8\pi}\left[I_0\left(\frac{K}{8\pi}\right)-I_1\left(\frac{K}{8\pi}\right)\right]\ . \tag{4.20}$$

The macroscopic "renormalized" elastic constants are

then given by

$$\mu_R(T)=\lim_{l\to\infty}\mu(l),\quad \lambda_R(T)=\lim_{l\to\infty}\lambda(l)\ . \tag{4.21a}$$

These formulas imply that μ_R and λ_R jump discontinuously to zero at T_m, preceded by a cusp singularity, and that

$$\lim_{T\to T_m^-}\frac{4\mu_R(\mu_R+\lambda_R)a_0^2}{(2\mu_R+\lambda_R)k_BT}=16\pi\ . \tag{4.21b}$$

Second, one finds that translational correlations decay above T_m, with a correlation length that diverges as T approaches T_m from above as

$$\xi_+(T)\approx a\exp(C/t^{\bar\nu})\ , \tag{4.22}$$

where

$$t=(T-T_m)/T_m,\quad \bar\nu=0.36963\ldots\ . \tag{4.23}$$

Although this correlation length controls the behavior of the structure factor above T_m, it also determines the density of free dislocations n_f,

$$n_f\approx\xi_+^{-2}\ . \tag{4.24}$$

It can be shown[5] that the dislocations unbind into a "hexatic" phase with quasi-long-range order in the bond-orientation field. The hydrodynamic description of this phase was described in Secs. II A and III B. The bond-orientation Frank constant $K_A(T)$ diverges as T approaches T_m from above,

$$K_A\sim n_f^{-1}\sim\xi_+^2\ . \tag{4.25}$$

C. Equations of motion

In order to study the dynamics near T_m, we must construct microscopic equations of motion for the time evolution of w_{ij}, δn_Δ, and $\vec g$ in the presence of moving dislocations. To determine these equations, we first define a Burgers-vector charge density,

$$\vec{\mathfrak{B}}(\vec r)=\sum_\nu\vec b^{(\nu)}\delta(\vec r-\vec R^{(\nu)})\ . \tag{4.26}$$

If the dislocations move around in space, we have a Burgers current of the ith component of dislocation charge in the jth direction, namely,

$$J_j^i=\sum_\nu b_i^{(\nu)}\frac{dR_j^{(\nu)}}{dt}\delta(\vec r-\vec R^{(\nu)})\ . \tag{4.27}$$

Conservation of the total Burgers charge requires an equation of continuity,

$$\frac{\partial\mathfrak{B}_i}{\partial t}=-\partial_jJ_j^i\ . \tag{4.28}$$

One further equation can be obtained by taking the time derivative of the integral of $w_{ij}(\vec r)$ around a large contour C enclosing a surface S

$$\frac{d}{dt}\oint_C w_{ij}dr_i=a_0\frac{d}{dt}\int_S d^2r\,\mathfrak{B}_j=-\int_S d^2r\,\partial_kJ_k^ja_0\ . \tag{4.29}$$

Transforming the surface integral to one over the contour C, we have

$$\oint_C\left(\frac{\partial w_{ij}}{\partial t}-a_0\epsilon_{ik}J_k^j\right)dr_i=0\ . \tag{4.30}$$

It follows that

$$\frac{\partial w_{ij}}{\partial t}-a_0\epsilon_{ik}J_k^j=-\partial_i\Xi_j\ , \tag{4.31}$$

where $\vec\Xi(\vec r)$ is a single-valued function of position. Inside a dislocation core, we expect that $\partial w_{ij}/\partial t$ is dominated by $\epsilon_{ik}J_k^j$, so that $\partial_i\Xi_j$ is unimportant. Away from all dislocation cores, however, J_k^i vanishes, and we must examine the form of Ξ_j.

Far away from dislocation cores, we can define a local defect current $\vec j^{\,\Delta}(\vec r)$ by

$$\vec j^{\,\Delta}(\vec r)=\frac{1}{m}\vec g(\vec r)-n_0\frac{\partial\vec u}{\partial t}\ . \tag{4.32}$$

For $\vec r$ on a cut K_ν, we interpret $\partial\vec u/\partial t$ to be the limiting value of this quantity as $\vec r$ approaches the cut, so there are no delta-function contributions arising from the motion of cuts. It follows, however, from (4.32), that away from these regions,

$$n_0\frac{\partial}{\partial t}w_{ij}=\frac{1}{m}\partial_ig_j-\partial_ij_j^\Delta\ . \tag{4.33}$$

Comparison with (4.31) then gives the identification,

$$\vec\Xi=-\frac{1}{n_0m}\vec g+\frac{1}{n_0}\vec j^{\,\Delta}\ , \tag{4.34}$$

so that it follows more generally that

$$\frac{\partial w_{ij}}{\partial t}=\frac{1}{n_0m}\partial_ig_j-\frac{1}{n_0}\partial_ij_j^\Delta+a_0\epsilon_{ik}J_k^j\ . \tag{4.35}$$

This result, which is fundamental to our subsequent analysis, may be checked by using it to evaluate $\partial n_\Delta/\partial t$. Since one always has

$$\frac{\partial n}{\partial t}=-\frac{1}{m_0}\vec\nabla\cdot\vec g\ , \tag{4.36}$$

we can combine (4.5) and (4.35) to find,

$$\frac{\partial n_\Delta}{\partial t}=\frac{\partial n}{\partial t}+n_0\frac{\partial w_{ii}}{\partial t}=-\vec\nabla\cdot\vec j^{\,\Delta}+n_0a_0\epsilon_{ik}J_k^i\ . \tag{4.37}$$

This equation identifies $\vec j^{\,\Delta}$ as the current associated with a defect density n_Δ which is conserved in the absence of dislocation currents. The term $\epsilon_{ik}J_k^i$ acts as a source which breaks this conservation law. Equation (4.37) reflects the well-known fact that a disloca-

tion moving perpendicular to its Burgers vector (in the climb direction) must act as a source or sink of vacancies and interstitials.

Our final equation of motion is just the conservation of momentum,

$$\partial g_i/\partial t = \partial_j \sigma_{ij} \ , \tag{4.38}$$

where σ_{ij} is to be determined. Equations (4.28), (4.35), (4.37), and (4.38) constitute the basic equations of motion of a solid imbedded with moving dislocations.

D. Constitutive relations

To complete our discussion of equations of motion on a microscopic scale, we must specify constitutive relations for $\vec{j}^{\Delta}$, σ_{ij}, and J_j^i. For $\vec{j}^{\Delta}$ and σ_{ij}, we simply extend the macroscopic relations of Sec. III C to microscopic length scales of order the vortex core diameter. For $\vec{j}^{\Delta}$, we write,

$$\begin{aligned}\vec{j}^{\Delta} &= -\Gamma_0 n_0^2 \vec{\nabla}(\delta F_{\rm mic}/\delta n_{\Delta}) + \vec{\eta}^{\Delta}(\vec{r},t) \\ &= -\Gamma_0 n_0 \vec{\nabla}(\chi_0^{-1}\delta n_{\Delta}/n_0 + \gamma_0 u_{ii}) + \vec{\eta}^{\Delta}(\vec{r},t) \ ,\end{aligned} \tag{4.39}$$

where $\vec{\eta}^{\Delta}(\vec{r},t)$ is a Gaussian Langevin noise source with mean zero and

$$\langle \eta_i^{\Delta}(\vec{r},t)\eta_j^{\Delta}(\vec{r}',t')\rangle = 2k_B T\Gamma_0 n_0^2 \delta_{ij}\delta(\vec{r}-\vec{r}')\delta(t-t') \ . \tag{4.40}$$

On the boundary we assume

$$\hat{n}\cdot\vec{j}^{\Delta} = n_0\Gamma_0^{(s)}(\chi_0^{-1}\delta n_{\Delta}/n_0 + \gamma_0 u_{ii} - \sigma_{ij}\hat{n}_i\hat{n}_j) \ , \tag{4.41}$$

in analogy to (3.33).

Away from the boundaries, the reversible part of the stress tensor is given by

$$\sigma_{ij}(\vec{r},t) = \delta F_{\rm mic}/\delta u_{ij} = 2\mu_0 u_{ij} + \tilde{\lambda}_0 u_{kk}\delta_{ij} + \gamma_0(\delta n_{\Delta}/n_0)\delta_{ij} \tag{4.42}$$

When the argument $\vec{r}$ approaches a point on the boundary of the sample, $\sigma_{ij}(\vec{r},t)$ must equal the external stress at that point. Strictly speaking there should be a dissipative term in σ_{ij}, analogous to Eq. (3.5), and a corresponding noise source. These terms are negligible, however, in the limit $k \to 0$, when dislocations are present.

To model dislocation motion producing the current density J_j^i, we consider a collection of M dislocations moving in the Peach-Koehler force.[24,33] We shall only consider dislocations whose Burgers vector $b^{(\nu)}$ is one of the six elementary lattice vectors of the triangular lattice. We designate these Burgers vectors with the symbol $b^{(\alpha)}$, with $\alpha = 1, 2, \ldots, 6$, and

$$\vec{b}^{(1)} = -\vec{b}^{(2)} = \begin{pmatrix} 1 \\ 0 \end{pmatrix} \ , \tag{4.43a}$$

$$\vec{b}^{(3)} = -\vec{b}^{(4)} = \begin{pmatrix} -\frac{1}{2} \\ \sqrt{3}/2 \end{pmatrix} \ , \tag{4.43b}$$

$$\vec{b}^{(5)} = -\vec{b}^{(6)} = \begin{pmatrix} -\frac{1}{2} \\ -\sqrt{3}/2 \end{pmatrix} \ . \tag{4.43c}$$

The position $\vec{R}^{(\nu)}$ of a Burgers vector of species α is assumed to obey a Langevin equation of the form

$$\frac{dR_i^{(\nu)}}{dt} = a_0\frac{D_{ij}^{(\alpha)}}{k_B T}(b_k^{(\alpha)}\epsilon_{lj} + b_l^{(\alpha)}\epsilon_{kj})[\sigma_{kl}(\vec{R}^{(\nu)}) + \bar{p}(\vec{R}^{(\nu)})\delta_{kl}] + \eta_i^{\nu}(t) \ , \tag{4.44}$$

where

$$\bar{p}(\vec{r}) = n_0\frac{\delta F_{\rm mic}}{\delta n_{\Delta}} = [\chi_0^{-1}n_0^{-1}\delta n_{\Delta}(\vec{r}) + \gamma_0 u_{ii}(\vec{r})] \ . \tag{4.45}$$

(Note: We shall continue to use the index ν, with $1 \le \nu \le M$, to label the various dislocations and the symbol α to designate which of the six species is involved. Our notation implies summation over Latin indices, which denote Cartesian components, but no summation over Greek indices.) The quantity $\bar{p}$ and the stress tensor σ_{kl} appearing in (4.44) should be interpreted as the average over a small circle enclosing $\vec{R}^{(\nu)}$, so that one excludes the singular angle-dependent contribution from the dislocation at $\vec{R}^{(\nu)}$. The $\{\eta_i^{\nu}(t)\}$ are fluctuating Gaussian noise sources with variances given by the diffusion tensor $D_{ij}^{(\alpha)}$,

$$\langle \eta_i^{\nu}(t)\eta_j^{\mu}(t')\rangle = 2D_{ij}^{(\alpha)}\delta(t-t') \ . \tag{4.46}$$

We assume there is no correlation between the noise sources for different dislocations.

The coefficient $D_{ij}^{(\alpha)}/k_B T$ in (4.44) is the mobility tensor by the Einstein relation. The factor multiplying the mobility is the "driving force" for the dislocation motion. The terms proportional to σ_{kl} give the usual "Peach-Koehler force,"[24,33] because of stress in the lattice; the term involving $\bar{p}$ arises because dislocation motion in the climb direction necessitates a change in the net number of defects (interstitials minus vacancies). Note that if the defect density n_{Δ} is allowed to reach thermal equilibrium in a

system under a uniform hydrostatic pressure, so that $\hat{n}\cdot\vec{j}^{\Delta}=0$ at the boundaries, then $(\sigma_{kl}+\bar{p}\delta_{kl})=0$ [cf. Eq. (4.41)]. We find then that there is no driving force to cause dislocation motion, as one would expect.

In an isotropic medium the diffusion tensor $D_{ij}^{(\alpha)}$ may be written,

$$D_{ij}^{(\alpha)}=D_{\parallel}b_i^{(\alpha)}b_j^{(\alpha)}+D_{\perp}(\delta_{ij}-b_i^{(\alpha)}b_j^{(\alpha)}) \quad . \tag{4.47}$$

Decomposing $d\vec{R}^{(\nu)}/dt$ into components parallel and perpendicular to $\vec{b}^{(\alpha)}$,

$$\left[\frac{d\vec{R}^{(\nu)}}{dt}\right]_i^{\parallel}=-a_0\frac{D_{\parallel}}{k_BT}b_i^{(\alpha)}b_j^{(\alpha)}(b_k^{(\alpha)}\epsilon_{lj}+b_l^{(\alpha)}\epsilon_{kj})\sigma_{kl}+(\vec{\eta}^{(\nu)})_i^{\parallel} \tag{4.48a}$$

and

$$\left[\frac{d\vec{R}^{(\nu)}}{dt}\right]_i^{\perp}=-a_0\frac{D_{\perp}}{k_BT}(\delta_{ij}-b_i^{(\alpha)}b_j^{(\alpha)})\times(b_k^{(\alpha)}\epsilon_{lj}+b_l^{(\alpha)}\epsilon_{kj})(\sigma_{kl}+\bar{p}\delta_{kl})+(\vec{\eta}^{(\nu)})_i^{\perp} \tag{4.48b}$$

we can identify $D_{\parallel}$ and $D_{\perp}$ as the glide and climb diffusion constants. Glide motion does not involve a change in particle number and proceeds more rapidly than climb motion, which can only occur by the absorption or emission of defects. Consequently, $D_{\perp}$ is usually much smaller than $D_{\parallel}$.[34]

To complete our microscopic description of dislocation motion we should take into account processes by which dislocations are created or destroyed, e.g., processes in which a pair of dislocations with opposite $\vec{b}$ are created or destroyed at some point of the system, processes where two dislocations combine to form a single dislocation whose Burgers vector is the sum of the first two, etc. These events change the number of dislocations of the six species ($\alpha=1,\ldots,6$) but do not change the total Burgers-vector density $\vec{\mathfrak{B}}(\vec{r})$. This latter quantity is all that will be needed in the following section.

To obtain a constitutive relation for the dislocation current density J_j^i, one must, in principle, solve the Fokker-Planck equation for the dislocation charge density following from (4.44). In practice, one can, in fact, guess the form for small deviations from equilibrium. The form of the dislocation current depends crucially on whether or not free dislocations exist in equilibrium. Indeed, the situation is not unlike that in electrodynamics, where very different conductivities are used to describe the current in metals and insulators. The precise form of J_j^i appropriate above and below the dislocation unbinding temperature T_m will be discussed in the next section.

V. DYNAMICS NEAR THE DISLOCATION UNBINDING TRANSITION

In this section we establish the relation between the microscopic description of a solid with dislocations, developed in the preceding chapter, and the macroscopic hydrodynamics of Sec. III. We show that in the long-wavelength limit the microscopic dynamics reduce to the macroscopic description of a solid or hexatic liquid crystal, depending on whether free dislocations are present or not.

We first consider the motion of free dislocations in detail and discuss the dynamics immediately above the melting temperature. In particular, we explain how the presence of free dislocations leads to a nonhydrodynamic decay of fluctuations in the defect density and a discontinuous change in the longitudinal sound velocity accompanied by an anomalous damping. We describe in addition how propagating transverse sound evolves into two diffusive modes in the hexatic-liquid-crystal phase.

To investigate the dynamics below the melting temperature we propose a simple approximation for the dynamic polarization of bound dislocation pairs.

A. Dynamics of free dislocations

In the hydrodynamic region above T_m, relaxation effects are dominated by free dislocations at a density $n_f\sim\xi_+^{-2}$. We define a smoothed Burgers-vector density

$$\langle\vec{\mathfrak{B}}(\vec{r},t)\rangle=\left\langle\sum_{\nu}\vec{b}^{(\nu)}\delta(\vec{r}-\vec{R}^{(\nu)})\right\rangle \tag{5.1}$$

as the average over the microscopic fluctuating noise $\vec{\eta}$. The quantity $\langle\vec{\mathfrak{B}}(\vec{r},t)\rangle$ can be written as the sum of the densities $\Gamma^{(\alpha)}(\vec{r},t)$ of dislocations with a particular Burgers vector $\vec{b}^{(\alpha)}$,

$$\langle\vec{\mathfrak{B}}(\vec{r},t)\rangle=\sum_{\alpha=1}^{6}b^{(\alpha)}\Gamma^{(\alpha)}(\vec{r},t) \quad . \tag{5.2}$$

$\Gamma^{(\alpha)}(\vec{r},t)$ obeys a Fokker-Planck equation of the form

$$\frac{\partial\Gamma^{(\alpha)}(\vec{r},t)}{\partial t}=-\partial_i j_i^{(\alpha)}(\vec{r},t)+Q^{(\alpha)}(\vec{r},t) \quad , \tag{5.3}$$

where $\vec{j}^{(\alpha)}$ is the current and $Q^{(\alpha)}$ the net production rate of dislocations of type $\vec{b}^{(\alpha)}$. Conservation of $\langle\vec{\mathfrak{B}}(\vec{r},t)\rangle$ implies

$$\sum_{\alpha=1}^{6}Q^{(\alpha)}(\vec{r},t)=0 \quad . \tag{5.4}$$

We shall neglect the detailed interactions between the dislocations, and assume that each dislocation diffuses independently and drifts under the influence of the macroscopic stress field $\sigma_{ij}(\vec{r})$ and "defect pres-

sure" $\bar{p}$. Using the Langevin equation (4.44) the current can then be written

$$j_i^{(\alpha)}(\vec{r},t) = -\frac{D_{ij}^{(\alpha)} a_0}{k_B T}\left(b_k^{(\alpha)}\epsilon_{lj} + b_l^{(\alpha)}\epsilon_{kj}\right) \times(\sigma_{kl}+\bar{p}\,\delta_{kl})\Gamma^{(\alpha)}(\vec{r},t) - D_{ij}^{(\alpha)}\partial_j\Gamma^{(\alpha)}(\vec{r},t) \quad . \tag{5.5}$$

In the present investigation we shall restrict ourselves to linear deviations from equilibrium. We can then replace the quantity $\Gamma^{(\alpha)}$ in the first term on the right-hand side of (5.5) by its equilibrium value $\frac{1}{6}n_f$. We shall also restrict ourselves, for the moment, to situations where the time scale for variations is long compared to the mean collision time between free dislocations, so that equilibrium between the different species is established and $\Gamma^{(\alpha)}(\vec{r},t) - \frac{1}{6}n_f$ is determined by the averaged Burgers-vector density $\langle\vec{\mathfrak{B}}(\vec{r},t)\rangle$:

$$\Gamma^{(\alpha)}(\vec{r},t) = \tfrac{1}{6}n_f + \tfrac{1}{3}b_j^{(\alpha)}\langle\mathfrak{B}_j(\vec{r},t)\rangle \quad . \tag{5.6}$$

We then find

$$\langle J_i^n\rangle = \sum_{\alpha=1}^{6} b_n^{(\alpha)} j_i^{(\alpha)} = -C_{ikl}^n(\sigma_{kl}+\bar{p}\,\delta_{kl}) - D_{il}^{nk}\partial_l\langle\mathfrak{B}_k\rangle \quad , \tag{5.7}$$

where

$$C_{ikl}^n = (n_f a_0/4k_B T)[(D_\parallel - D_\perp)\delta_{ik}\epsilon_{ln} + (D_\parallel + 3D_\perp)\delta_{nk}\epsilon_{li}] \quad , \tag{5.8a}$$

$$D_{il}^{nk} = \tfrac{1}{4}(D_\parallel - D_\perp)(\delta_{in}\delta_{lk} + \delta_{ik}\delta_{ln}) + \tfrac{1}{4}(D_\parallel + 3D_\perp)\delta_{il}\delta_{nk} \quad . \tag{5.8b}$$

For purposes of illustration we shall assume a simplified model, in which $D_\parallel = D_\perp \equiv D$. In this case Eq. (5.7) may be written

$$\langle J_i^n(\vec{r},t)\rangle = -(Da_0 n_f/k_B T)\epsilon_{li}(\sigma_{nl}+\bar{p}\,\delta_{nl}) - D\,\partial_i\langle\mathfrak{B}_n(\vec{r},t)\rangle \quad . \tag{5.9}$$

By means of the conservation law (4.28), the Burgers-vector density $\langle\vec{\mathfrak{B}}\rangle$ may be expressed in terms of the current $\langle J_i^n\rangle$. After a Fourier transformation, one finds

$$\langle J_i^n(\vec{k},\omega)\rangle = -\frac{Da_0 n_f}{k_B T}\epsilon_{li}(\sigma_{nl}+\bar{p}\,\delta_{nl}) + ik_i\epsilon_{lj}k_j(\omega+iDk^2)^{-1} \times\frac{D^2 a_0 n_f}{k_B T}(\sigma_{nl}+\bar{p}\,\delta_{nl}) \quad . \tag{5.10}$$

(The general case $D_\parallel \neq D_\perp$ is discussed in Appendix B.) With $\langle J_i^n\rangle$ expressed in terms of σ_{ij} and $\bar{p}$, the system of dynamic equations closes and we can proceed to study the dynamics immediately above T_m.

B. Transverse excitations above T_m

The set of equations (4.28), (4.35), (4.37), and (4.38) can easily be separated into sets of three and five equations decoupled from each other. The former set describes transverse excitations of momentum and displacement field coupled to the longitudinal Burgers-vector component. For example, if we take $\vec{k}$ in the x direction, the nonzero variables will be w_{xy}, w_{yx}, g_y, $\langle\mathfrak{B}_x\rangle$, $\langle J_x^x\rangle$, and $\langle J_y^y\rangle$. The equations of motion are

$$-i\omega\langle\mathfrak{B}_x\rangle = -ik\langle J_x^x\rangle \quad , \tag{5.11}$$

$$ikw_{yx} = \langle\mathfrak{B}_x\rangle a_0 \quad , \tag{5.12a}$$

$$-i\omega w_{xy} = (ik/n_0 m)g_y + \langle J_y^y\rangle a_0 \quad , \tag{5.12b}$$

$$-i\omega g_y = ik\mu_0(w_{xy}+w_{yx}) = ik\sigma_{xy} \quad . \tag{5.13}$$

The equation for the time derivative of w_{yx} is redundant with (5.12a) and (5.11) and has not been exhibited. With the approximation of a diagonal diffusion tensor we have

$$\langle J_y^y\rangle = -(\nu_0/a_0)\sigma_{xy} \quad , \tag{5.14a}$$

$$\langle J_x^x\rangle = (\nu_0/a_0)\sigma_{xy}(1+iDk^2/\omega)^{-1} \quad , \tag{5.14b}$$

where it has been convenient to define

$$\nu_0 = (D/k_B T)n_f a_0^2 \sim \xi_+^{-2} \quad . \tag{5.14c}$$

Solving (5.11)–(5.13) in the limit $(k\xi_+) \ll 1$, one finds two diffusive modes and one relaxational mode with eigenfrequencies

$$\omega_1 = -ik^2 1/2n_0 m\nu_0 \sim -i(k\xi_+)^2 \quad , \tag{5.15}$$

$$\omega_2 = -iDk^2 \quad , \tag{5.16}$$

$$\omega_3 = -i2\mu_0\nu_0 \sim -i\xi_+^{-2} \quad . \tag{5.17}$$

The relaxational mode exhibits critical slowing down with the same temperature dependence as ξ_+^{-2}, and describes the decay of fluctuations in the density of free dislocations. The two diffusive modes describe coupled excitations of the transverse momentum and the bond-orientation field. One of the diffusion coefficients diverges like ξ_+^2.

It is instructive to compare these results with hexatic liquid-crystal hydrodynamics which was discussed in Sec. III B. There we found two eigenfrequencies with a k^2 dispersion, but it was impossible to discriminate between propagating and purely diffusive modes. The results (5.15)–(5.17) show that close to T_m the latter case is realized. In Appendix C, we

compare the hydrodynamic equations more closely with Eqs. (5.11)–(5.13), and we conclude that η diverges like ξ_+^2, and κ remains finite at T_m. In terms of the actual parameters of our model, we find

$$\eta = 1/(2\nu_0) \ , \tag{5.18}$$

$$\kappa = \tfrac{1}{2} D \ , \tag{5.19}$$

$$K_A = D/\nu_0 = k_B T/n_f a_0^2 \ . \tag{5.20}$$

Note that K_A also diverges like ξ_+^2, as predicted by the static theory.[5]

If we allow for different diffusion constants for climb and glide, the results (5.15)–(5.20) are slightly modified. The single diffusion constant D must be replaced by the quantity $(\frac{1}{2}D_{\parallel}+\frac{1}{2}D_{\perp})$ where it appears in Eqs. (5.14c) and (5.20), by the quantity $D_{\parallel}$, where D appears in (5.19) and by the quantity $(\frac{3}{4}D_{\parallel}+\frac{1}{4}D_{\perp})$ where D appears in (5.16) and in (5.21) below. (See Appendix C for details.)

At wave numbers $k > \xi_+^{-2}$ above T_m the dislocation density again decouples and shows purely diffusive motion

$$\omega = -ik^2 D \ . \tag{5.21}$$

In addition we recover the propagating shear waves of the solid phase for $k >> \xi_+^{-2}$. However, the polarization of bound pairs becomes important in this region. We expect a renormalization of the sound velocity, as well as additional contributions to the damping of sound waves. This point will be discussed in Sec. V D.

It is interesting to contrast these results with those suggested by straightforward application of the dynamic scaling hypothesis.[23,35] Since the shear modulus is finite even at T_m, we would expect propagating shear waves with a linear dispersion at finite wave vectors above T_m provided $k\xi_+ \gtrsim 1$. If the characteristic frequencies $\omega_t^{\pm}(k\xi_+)$ of transverse excitations were to scale, it would then have to be with dynamic scaling exponent $z=1$, $\omega_t^{\pm} = k\,\Omega_{\pm}(k\xi_+)$. In view of the expected hexatic behavior described in Sec. III B, it is very tempting to assume propagating hydrodynamic shear excitations above T_m with the dispersion relations (3.22). Dynamic scaling would predict that the real part of $\omega_t^{\pm}$ dominates near T_m with $\tilde{c}_t \propto \xi_+$. The analysis of this subsection, however, shows that this is *not* the case. The dynamic scaling hypothesis fails near T_m.

C. Longitudinal modes

We now proceed to solve the five coupled equations for longitudinal excitations near T_m. Choosing k in the x direction, the nonzero variables are w_{xx}, w_{yy}, $\langle \mathfrak{B}_y \rangle$, g_x, $\langle J_x^y \rangle$, $\langle J_y^x \rangle$, and δn_{Δ}. The equations of motion read

$$-i\omega \langle \mathfrak{B}_y \rangle = -ik \langle J_x^y \rangle \ , \tag{5.22}$$

$$w_{yy} = -i(a_0/k)\langle \mathfrak{B}_y \rangle \ , \tag{5.23a}$$

$$-i\omega w_{xx} = i(k/n_0 m) g_x - \Gamma k^2 [\chi_0^{-1}\delta n_{\Delta}/n_0 + \gamma_0 (w_{xx}+w_{yy})] + a_0 \langle J_y^x \rangle \ , \tag{5.23b}$$

$$-i\omega g_x = ik\,[2\mu_0 w_{xx} + \tilde{\lambda}_0 (w_{xx}+w_{yy}) + \gamma_0 \delta n_{\Delta}/n_0] \ , \tag{5.24}$$

$$-i\omega \delta n_{\Delta}/n_0 = -\Gamma k^2 [\chi_0^{-1}\delta n_{\Delta}/n_0 + \gamma_0 (w_{xx}+w_{yy})] + a_0 (\langle J_y^x \rangle - \langle J_x^y \rangle) \ . \tag{5.25}$$

With the aid of (5.10) the required components of the Burgers-vector current can be worked out

$$\langle J_y^x \rangle = -(\nu_0/a_0)(\sigma_{xx}+\bar{p}) \ , \tag{5.26a}$$

$$\langle J_x^y \rangle = (\nu_0/a_0)(\sigma_{yy}+\bar{p})(1+iDk^2/\omega)^{-1} \ , \tag{5.26b}$$

where we have assumed a diagonal diffusion tensor. The equation of motion for the redundant variable w_{yy} has not been displayed.

The free dislocations present above T_m provide a local source or sink for the defect density and allow a stress to relax by the process of dislocation motion. The decay of fluctuations in the defect density and the strain field becomes nonhydrodynamic, as is evident from the relaxational terms proportional to $\nu_0 \sim n_f$ in (5.23b) and (5.25). However, the total number density, $\delta n = -n_0 u_{ii} + \delta n_{\Delta}$, as well as the longitudinal component of the momentum density are still conserved. We therefore expect two hydrodynamic and two relaxational eigenfrequencies. Solving (5.22)–(5.25) in the region $(k\xi_+) << 1$ one finds for the latter

$$\omega_1 = -2i\mu_0\nu_0 \sim \xi_+^{-2} \tag{5.27}$$

and

$$\omega_2 = -2i\nu_0(\mu_0 + \tilde{\lambda}_0 + \chi_0^{-1} + 2\gamma_0) \sim \xi_+^{-2} \ . \tag{5.28}$$

Both modes exhibit critical slowing down with the temperature dependence of ξ_+^{-2}. The other two modes are longitudinal sound excitations with dispersion relations

$$\omega_l^{\pm} = \pm c_l k - iD_l k^2 \tag{5.29}$$

with

$$D_l \propto \frac{1}{n_f} \propto \xi_+^2 \ , \tag{5.30a}$$

$$m n_0 c_l^2 = \frac{\mu_0 + \tilde{\lambda}_0 - \gamma_0^2 \chi_0}{1 + \chi_0 (2\gamma_0 + \mu_0 + \tilde{\lambda}_0)} \equiv B_0 \ . \tag{5.30b}$$

Comparing (5.30b) with Eq. (2.23), we see that B_0 is equal to the bulk modulus of the solid within the current approximation, where we neglect the renormalization due to bound dislocations. (In fact, we expect the bulk modulus and all its derivatives to vary continuously as one passes through T_m from the solid to the hexatic phase,[5] so that B_0 is a good approximation to the bulk modulus in both phases.)

The sound velocity is determined by the bulk modulus, since above T_m fluctuations in δn_Δ now relax *rapidly* compared to the inverse sound frequency, due to the presence of free dislocations and since the shear modulus is zero. Thus, there is indeed a discontinuous change in the longitudinal sound velocity at the dislocation unbinding transition as was suggested by the results of Sec. III. The discontinuous change in the real part of $\omega_l^{\pm}$ is accompanied by a sound-wave damping constant D_l diverging like ξ_+^2. Such a remarkable temperature dependence should be readily detectable in sound-absorbtion experiments.

The eigenfrequencies (5.29) and (5.30) correspond to the longitudinal hydrodynamic excitations (3.16)–(3.18) found in hexatic liquid crystals. The divergent damping constant D_l implies a divergence of $\eta+\zeta$ near T_m in the liquid-crystal phase.

In the more general case of different glide and climb diffusion constants the relaxation rates $\omega_{1,2}$ are changed to

$$\omega_1 = -i(D_\parallel + D_\perp)\mu_0 n_f a_0^2/k_B T \sim \xi_+^{-2} \ , \tag{5.31}$$

$$\omega_2 = -i2D_\perp(\mu_0+\tilde{\lambda}_0+\chi_0^{-1}+2\gamma_0)n_f a_0/k_B T \sim \xi_+^{-2} \ . \tag{5.32}$$

Solving (5.22)–(5.26) in the region $(k\xi_+) \gtrsim 1$ above T_m we recover the solid hydrodynamic modes of Sec. III C, and find in particular that the speed of longitudinal sound is $c_l = [(2\mu_0+\tilde{\lambda}_0)/n_0 m]^{1/2}$. The dislocation density decouples and shows purely diffusive behavior

$$\omega = -i\tfrac{1}{4}(D_\parallel + 3D_\perp)k^2 \ . \tag{5.33}$$

However, just as in the case of the transverse excitations, the polarization of bound dislocation pairs must be taken into account to describe this region completely.

D. Dynamics of bound dislocation pairs

Thus far we have only considered the effect of free dislocations, which dominate the dynamics above T_m in the long wavelength, low-frequency region. Just above T_m for short wavelengths $(k\xi_+) \gtrsim 1$, as well as in the hydrodynamic region below T_m the dynamic polarization of bound dislocation pairs becomes important.

We restrict ourselves for the moment to a situation below T_m, where no free dislocations are present and consider a bound pair in an applied oscillating stress field $\sigma_{ij}(\omega)$. The stress tends to polarize the pairs, giving rise to a Burgers-vector current J_j^i. It is convenient to introduce a symmetrized current

$$\tilde{J}_{ij} = (\epsilon_{ik}J_k^j + \epsilon_{jk}J_k^i) \ , \tag{5.34}$$

which, in linear approximation, is proportional to the driving field $\sigma_{ij}+\bar{p}\delta_{ij}$,

$$\tilde{J}_{ij}(\omega) = i\omega\chi_{ijkl}(\omega)[\sigma_{kl}(\omega)+\bar{p}(\omega)\delta_{kl}] \ . \tag{5.35}$$

Having separated out a factor $i\omega$ from the generalized susceptibility $\chi_{ijkl}(\omega)$, the latter should be finite at zero frequency, if there are no free dislocations and therefore no current in a static field. In fact, the situation is quite analogous to a more familiar problem in electrodynamics: the dynamic polarization of bound charges in an insulator.

In principle $\chi_{ijkl}(\omega)$ can be calculated from the Fokker-Planck equation for the number density of dislocation pairs, as was done by Ambegaokar and Teitel[36] for the dynamics of vortex pairs in superfluid films. Since such an analysis is rather involved due to the coupling between different Burgers vectors, we limit ourselves to a simple approximation for $\chi_{ijkl}(\omega)$.

Let us consider in particular the response to a pure shear $\sigma_{xy}(\omega)$, which can be relaxed by dislocation glide and climb. We assume that these processes can be characterized by two relaxation rates $\nu_\parallel(r)$ and $\nu_\perp(r)$, which we estimate to be of order $D_\parallel r^{-2}$ and $D_\perp r^{-2}$. Both processes can be approximately described by a two-pole function

$$\chi_{xyxy}(\omega) \simeq \int_{a_0}^{\infty} dr\, \tilde{\chi}(r)\left[\frac{D_\parallel r^{-2}}{-i\omega+D_\parallel r^{-2}} + \frac{D_\perp r^{-2}}{-i\omega+D_\perp r^{-2}}\right] \equiv \chi_\mu(\omega) \ . \tag{5.36}$$

The diffusion of dislocation pairs tends to relax the strain field u_{ij} according to (5.12a) and (5.12b). Applying Eq. (4.35) in the limit $k \to 0$, we have

$$-i\omega(w_{xy}+w_{yx}) = -i\omega 2u_{xy} = i\omega\chi_{xyxy}\sigma_{xy} \ . \tag{5.37}$$

To ensure the correct static response we choose

$$\chi_{xyxy}(\omega=0) = 2\int_{a_0}^{\infty} dr\, \tilde{\chi}(r) = \int_{a_0}^{\infty} dr\, \frac{d\mu^{-1}(r)}{dr} \ , \tag{5.38}$$

where $d\mu^{-1}/dr$ is determined by (4.19) with $r = a_0 e^l$.

To study the effect of bound dislocation pairs on propagating transverse sound, one should investigate the response to a nonuniform applied stress and generalize (5.35) to finite wave numbers. As in the case of third sound in superfluid films[26] it is possible to approximate $\chi_\mu(k,\omega)$ by $\chi_\mu(k=0,\omega)$ in the regions

of interest here. To see this, we have to estimate the characteristic length scales for the diffusion of dislocations and defects and compare it to the wavelength of transverse sound. During one period of sound a dislocation can glide over a distance $\delta_{\parallel} \sim (D_{\parallel}/\omega)^{1/2}$ and climb a distance $\delta_{\perp} \sim (D_{\perp}/\omega)^{1/2}$. In the hydrodynamic region $\delta_{\parallel}$ and $\delta_{\perp}$ are much smaller than the wavelength of transverse sound $\lambda = c_t/\omega$, which is therefore perceived as an effectively uniform perturbation by dislocations.

Climb motion is necessarily accompanied by a local change in the defect density $n_{\Delta}(\vec{r})$. However, a uniform shear leaves the macroscopic defect-density unchanged. Using the same arguments as above, one can show that transverse sound appears as an effectively uniform shear for defects, provided ω is sufficiently small. Therefore, defect diffusion and transverse sound decouple in the hydrodynamic region below T_m and above T_m for $(k\xi_+) >> 1$.

We therefore approximate the contribution of bound dislocation pairs to the current $\tilde{J}_{xy}$ by

$$\tilde{J}_{xy}(\vec{q},\omega) \simeq i\omega\chi_{\mu}(\omega)\sigma_{xy}(\vec{q},\omega) \ . \tag{5.39}$$

Inserting this expression into (5.11) and (5.12) and solving for $T < T_m$, where no free dislocations are present, one finds the following dispersion relation for transverse sound

$$k^{\pm}(\omega) = \pm[\epsilon_{\mu}(\omega)]^{1/2}\omega/c_t \tag{5.40}$$

with

$$\epsilon_{\mu}(\omega) = 1 + \chi_{\mu}(\omega)\mu_0 \ . \tag{5.41}$$

Below T_m the imaginary part of $\epsilon_{\mu}(\omega)$ is much smaller than its real part. Expanding (5.40) in $\mathrm{Im}\epsilon_{\mu}(\omega)/\mathrm{Re}\epsilon_{\mu}(\omega)$ one finds

$$k^{\pm}(\omega) = \pm\frac{\omega}{c_t(\omega)} + \frac{1}{2}i\frac{\omega}{c_t(\omega)}\frac{\mathrm{Im}\epsilon_{\mu}(\omega)}{\mathrm{Re}\epsilon_{\mu}(\omega)} \tag{5.42}$$

with

$$c_t(\omega) = \frac{c_t}{\mathrm{Re}\epsilon_{\mu}(\omega)} = \frac{1}{mn_0}\frac{\mu_0}{\mathrm{Re}\epsilon_{\mu}(\omega)} \ . \tag{5.43}$$

The real part of $\epsilon_{\mu}(\omega)$ renormalizes the sound velocity and the imaginary part determines the damping. To discuss the damping of transverse sound due to bound dislocation pairs, we estimate the real and imaginary part of $\epsilon_{\mu}(\omega)$. Below T_m we follow Ref. 26 and introduce a correlation length $\xi^{-}(T)$, which close to T_m diverges like $\xi^{-}(T) \sim \exp(c/|T - T_m|^{\bar{\nu}})$, where c is a nonuniversal constant and $\bar{\nu}$ is given by (4.23). For $r > \xi^{-}$ one finds

$$\mu_R^{-1} - \mu^{-1}(r) \sim r^{(4-K_R/4\pi)} \ . \tag{5.44}$$

At T_m and for length scales $r < \xi^{-}$ below T_m we use the results of Ref. 5 for the recursion relations in the vicinity of $K = 16\pi$. There a small deviation $x(l)$ was defined

$$K^{-1}(l) = (1/16\pi)[1 + x(l)] \tag{5.45}$$

in terms of which the recursion relation for μ^{-1} is approximately given by

$$\frac{d\mu^{-1}}{dl} \sim x^2(l) \sim \frac{1}{(1+\tilde{c}l)^2} \ , \tag{5.46}$$

where $\tilde{c}$ is another nonuniversal constant.

Estimating $\mathrm{Re}\epsilon_{\mu}(\omega)$ and $\mathrm{Im}\epsilon_{\mu}(\omega)$ as in Ref. 26 and expanding (5.42) in the ratio $\mathrm{Im}\epsilon_{\mu}(\omega)/\mathrm{Re}\epsilon_{\mu}(\omega)$ one finds for $T < T_m$,

$$\omega_{\pm}(k) = \pm c_t(0)k - iD_t k k^{(K_R/8\pi - 2)} \ , \tag{5.47}$$

where near T_m, $(K_R/8\pi - 2) \sim |T - T_m|^{\bar{\nu}}$. D_t can be related to the climb and glide diffusion constants. We have neglected dissipative couplings in the hydrodynamic equations (4.42), which would give additional contributions to the damping proportional to k^2.

At T_m we find with the help of (5.46)

$$\omega = \pm c_t(0)k - iD_t' k/\ln^2(ka_0) \tag{5.48}$$

so that transverse sound is indeed propagating in the long-wavelength limit.

For $T > T_m$ and $(k\xi_+) >> 1$, $\epsilon_{\mu}(\omega)$ is effectively constant and can be replaced by its value at T_m, $\epsilon_{\mu}(\omega) \approx \epsilon_c = \mu_0/\mu_R(T_m^{-})$. Solving (5.11)–(5.13) in this approximation we recover the results of Sec. III C.

VI. HEXATICS WITH DISCLINATIONS

The hydrodynamic description of the hexatic phase described in Sec. III B should be applicable (neglecting long-time tails) for small wave vectors $\vec{q}$ anywhere between T_m and T_i. Indeed, since $K_A(T)$ is finite just below T_i, we expect that qualitatively similar hydrodynamic modes will persist even *above* T_i, provided $q \geq \xi_{\psi}^{-1}$. A finite density $n_f^{(6)} \sim \xi_{\psi}^{-2}$ of free disclinations destroys quasi-long-range order in θ above T_i, however, and reduces the number of hydrodynamic modes which persist as q tends to zero. To study this further we must incorporate disclinations into a microscopic dynamical description. This will be done in close analogy to the treatment of third sound in superfluid films by Ambegaokar *et al.*[26] with, however, qualitatively different results.

A. Microscopic model: A hexatic with disclinations

To exploit the analogy with superfluidity, we consider the dynamics of a microscopic vector field analogous to the superfluid velocity,

$$\vec{v}_h(\vec{r},t) \equiv \vec{\nabla}\theta(\vec{r},t) \ , \tag{6.1}$$

rather than the dynamics of the bond-angle field itself. In the presence of disclinations, $\theta(\vec{r},t)$ can be made single valued only by introducing jump discontinuities across cuts in the xy plane. The gradient of $\theta(\vec{r},t)$ is a smooth function of $\vec{r}$ except at the isolated points occupied by disclinations. It is defined to exclude the delta-function contribution at the discontinuities of $\theta(\vec{r},t)$. Since the integral of $\vec{v}_h$ around any closed path must be $\frac{1}{3}\pi$ times the enclosed integer "disclinicity," we must have

$$\vec{\nabla} \times \vec{v}_h(\vec{r},t) = S(\vec{r},t) \ , \tag{6.2}$$

where $S(\vec{r},t)$ is a disclination charge density,

$$S(\vec{r},t) = \tfrac{1}{3}\pi \sum_\nu s_\nu \delta(\vec{r} - \vec{R}^{(\nu)}(t)) \ . \tag{6.3}$$

In Eq. (6.3), the summation is over disclinations at points $\{\vec{R}^{(\nu)}(t)\}$ carrying "disclinicity" $s_\nu = 0, \pm 1, \ldots$. We can also define a disclination current density

$$\vec{J}_6(\vec{r},t) = \tfrac{1}{3}\pi \sum_\nu s_\nu \frac{d\vec{R}^{(\nu)}(k)}{dt} \delta(\vec{r} - \vec{R}^{(\nu)}(t)) \ . \tag{6.4}$$

Because disclinations can be created or destroyed only in pairs of opposite sign or at boundaries, we have a continuity equation

$$\frac{\partial S}{\partial t} + \vec{\nabla} \cdot \vec{J}_6 = 0 \ . \tag{6.5}$$

Since Eqs. (6.5) and (6.2) can be combined to read

$$\vec{\nabla} \times \left(\frac{d\vec{v}_h}{dt} - \hat{z} \times \vec{J}_6 \right) = 0 \ , \tag{6.6}$$

the quantity $d\vec{v}_h/dt - \hat{z} \times \vec{J}_6$ must be the gradient of a smooth scalar function without singularities. To recover the results of Sec. III B in the absence of disclination currents, we take this function to be the right-hand side of Eq. (3.14) and find

$$\frac{\partial \vec{v}_h}{\partial t} = \frac{1}{2mn_0} \vec{\nabla}(\epsilon_{ij}\partial_i g_j) + \kappa \vec{\nabla}(\vec{\nabla} \cdot \vec{v}_h) + \hat{z} \times \vec{J}_6 \ . \tag{6.7}$$

The two remaining hydrodynamic equations are unchanged,

$$\frac{\partial \delta n}{\partial t} = -\frac{1}{m} \vec{\nabla} \cdot \vec{g} \ , \tag{6.8}$$

$$\frac{\partial \vec{g}}{\partial t} = -\tfrac{1}{2} K_A^0 (\hat{z} \times \vec{\nabla})(\vec{\nabla} \cdot \vec{v}_h) - \frac{B}{n_0} \vec{\nabla} \delta n + \frac{\eta}{mn_0} \nabla^2 \vec{g} + \frac{\zeta}{mn_0} \vec{\nabla}(\vec{\nabla} \cdot \vec{g}) \ . \tag{6.9}$$

Note that the "conservation of $\vec{v}_h$" is broken explicitly by disclination currents. Below T_i, where disclinations are bound and $\vec{J}_6$ vanishes at long wavelengths, we recover our previous hydrodynamic description. The microscopic field $\theta(\vec{r},t)$ can then be replaced by the macroscopic quantity $\Theta(\vec{r},t)$, if we neglect renormalizations due to bound pairs.

B. Interacting disclinations in equilibrium

The microscopic probability distribution, to which our hexatic equations of motion must relax, is proportional to $\exp(-F_H/k_BT)$, where

$$F_H = F_L + \delta F_H \ . \tag{6.10}$$

Here, F_L is the usual liquid-free energy Eq. (2.1), and

$$\delta F_H = \tfrac{1}{2} K_A^0 \int d^2r (\vec{\nabla}\theta)^2 \ . \tag{6.11}$$

Decomposing $\theta(\vec{r})$ into a smoothly varying part $\phi(\vec{r})$ and a part due to disclinations, we can rewrite (6.11) in the form

$$\delta F_H = \tfrac{1}{2} K_A^0 \int d^2r (\vec{\nabla}\phi)^2 - \frac{\pi K_A^0}{36} \sum_{\vec{r} \neq \vec{r}'} s(\vec{r}) s(\vec{r}') \ln \left| \frac{\vec{r} - \vec{r}'}{a} \right| + E_c^{(6)} \sum_{\vec{r}} s^2(\vec{r}) \ , \tag{6.12}$$

where $E_c^{(6)}$ is a disclination core energy. The vectors $\vec{r}$ run over the sites of a lattice whose only physical significance is to provide a short-distance cutoff.

The statistical mechanics of (6.12) is isomorphic to the scalar Coulomb-gas model of superfluidity and XY magnetism treated by Kosterlitz,[37] except that disclinations play the role of vortices. Taking over his renormalization equations to the present situation, we have

$$\frac{d(K_A^0(l))^{-1}}{dl} = 144\pi^3 y_6^2(l) \ , \tag{6.13}$$

$$\frac{dy_6(l)}{dl} = \left(2 - \frac{\pi}{36} K_A^0(l) \right) y_6(l) \ , \tag{6.14}$$

where

$$y_6(0) = \exp(-E_c^{(6)}/k_BT) \tag{6.15}$$

and $K_A^0(l)$ and $y_6(l)$ describe "partially dressed" couplings with fluctuations on scales a to ae^l integrated out. Here a is the disclination core diameter.

Using these results, it is straightforward to show[5] that the renormalized Frank constant $K_A(T)$ is

$$K_A(T) = \lim_{l \to \infty} K_A^0(l) \ , \tag{6.16}$$

and that disclinations unbind at temperature T_i, such

that

$$\lim_{T\to T_i} K_A(T) = 72k_B T_i/\pi \ , \tag{6.17}$$

driving a transition into an isotropic liquid phase. The Frank constant K_A vanishes above this temperature. Bond-orientation correlations then decay exponentially, with a diverging correlation length,

$$\xi_\psi(T) \sim \exp(b/|T-T_i|^{1/2}) \ , \tag{6.18}$$

just above T_i. At all temperatures in the hexatic phase, one has the result quoted in the Introduction,

$$\eta_6(T) = 18k_B T/\pi K_A(T) \ . \tag{6.19}$$

Just above T_i, the density $n_f^{(6)}$ of free dislocations can be expressed in terms of (6.18),

$$n_f^{(6)} \approx \xi_\psi^{-2}(T) \ . \tag{6.20}$$

C. Equations of motion for disclinations

Physically, we expect that disclinations will move in response to inhomogeneities in the bond-angle field. To proceed further, we need a model of disclination motion which allows us to calculate the disclination currents produced in the presence of a finite $\vec{v}_h$. Following arguments which lead to the Magnus force on vortices[38] and the Peach-Koehler force on dislocations,[33] we ask for the force on a disclination at $\vec{R}^{(\nu)}$ with charge s_ν in the presence of a "velocity" field $\vec{v}_h(\vec{r},t)$. The requirement that this force gives the correct energy for a disclination pair leads to a disclination force

$$\vec{F}_6(\vec{R}^{(\nu)},t) = -\tfrac{1}{3}\pi K_A^0 s_\nu \hat{z}\times\vec{v}_h(\vec{R}^{(\nu)},t) \ . \tag{6.21}$$

We now associate a simple Langevin equation for the disclination position with this force, namely,

$$\frac{d\vec{R}^{(\nu)}}{dt} = -s_\nu \frac{\pi K_A^0 D_6}{3k_B T}\hat{z}\times\vec{v}_h(\vec{R}^{(\nu)},t) + \vec{\eta}^{(\nu)}(t) \ , \tag{6.22}$$

where D_6 is a diffusion constant, and the $\vec{\eta}_\nu(t)$ are fluctuating Gaussian noise sources with variance

$$\langle \eta_i^{(\mu)}(t)\eta_j^{(\nu)}(t')\rangle = 2D_6\delta_{ij}\delta_{\mu\nu}\delta(t-t') \ . \tag{6.23}$$

Equation (6.22) represents diffusive disclination motion with a mean velocity proportional to the magnus force $\vec{F}_6$. Just as in Ref. 26, these equations could be used in conjunction with (6.7) to study the response to homogeneous, time-dependent perturbations. Here, we are interested instead in hydrodynamic excitations at long wavelengths in the presence of a dilute gas of free disclinations.

To study this situation further, we consider the Fokker-Planck equation implied by (6.22) for the disclination charge density $S_{\rm free}(\vec{r},t)$ averaged over a small hydrodynamic volume, which must be of the form

$$\frac{\partial S_{\rm free}}{\partial t} + \vec{\nabla}\cdot\vec{J}_{6,\rm free} = 0 \ , \tag{6.24}$$

to ensure conservation of $S_{\rm free}$. For small deviations from equilibrium, the current of free disclinations must take the form

$$J_{6,\rm free}(\vec{r},t) = \gamma_0\hat{z}\times\vec{v}_h(\vec{r},t) - D_6\vec{\nabla}S_{\rm free}(\vec{r},t) \ , \tag{6.25}$$

where D_6 is the disclination diffusion constant and γ_0 is proportional to a disclination mobility.[39] We require that zero-current results from the equilibrium distribution $S_0(r)$ associated with a uniform vector field $\vec{v}_h^0$. This quantity is

$$S_0(\vec{r}) \approx n_f^{(6)}\exp(-\vec{F}_6^0\cdot\vec{r}/k_B T) \ , \tag{6.26}$$

where $n_f^{(6)}$ is the density of free disclinations, and

$$\vec{F}_6^0 = -\tfrac{1}{3}\pi K_A^0 s_\nu(\hat{z}\times\vec{v}_h^0) \ . \tag{6.27}$$

This constraint of zero current gives the Einstein relation

$$\gamma_0 = \pi K_A^0 D_6 n_f^{(6)}/3k_B T \ . \tag{6.28}$$

In what follows, we assume that D_6 remains finite near T_i, so that the dominant temperature dependence in γ_0 comes from $n_f^{(6)} \approx \xi_\psi^{-2}$.

D. Dynamics above T_i

In order to use the results for $S_{\rm free}$ and $\vec{J}_{6,\rm free}$ derived above, we first break the currents and charges in Eqs. (6.2) and (6.7) into free and bound parts, and assume that bound disclinations can be taken into account by a bound dielectric constant ϵ_c. Taking over the standard treatment of free and bound charges in, e.g., Maxwell's equations,[40] these equations become

$$\epsilon_c\vec{\nabla}\times\vec{v}_h = S_{\rm free} \ , \tag{6.29}$$

$$\epsilon_c\frac{\partial\vec{v}_h}{\partial t} = \frac{1}{2mn_0}\vec{\nabla}(\epsilon_{ij}\partial_i g_j) + \lambda\vec{\nabla}(\vec{\nabla}\cdot\vec{v}_h) + \hat{z}\times\vec{J}_{6,\rm free} \ , \tag{6.30}$$

while (6.8) and (6.9) are unchanged.

Passing to Fourier transformed variables $\vec{v}_h(\vec{q},\omega)$, $S(\vec{q},\omega)$, etc., we can close the system of equations (6.30), (6.8), and (6.9) by first solving (6.24) for

$$S_{\rm free}(\vec{q},\omega) = \frac{i\gamma_0\vec{q}\times\vec{v}_h(\vec{q},\omega)}{-i\omega + D_6 q^2} \ . \tag{6.31}$$

One then finds from (6.25) that

$$J^i_{6,\rm free}(\vec{q},\omega) = \gamma_0\left(\epsilon_{ij} - \frac{D_6 q_i q_l \epsilon_{lj}}{-i\omega + D_6 q^2}\right)v_h^j(\vec{q},\omega) \ . \tag{6.32}$$

Inserting this into (6.30), and projecting the equations of motion onto the longitudinal and transverse parts of $\vec{v}_h$ and $\vec{g}$, we find five distinct eigenfrequencies. The transverse momentum and longitudinal part of $\vec{v}_h$ couple to give the analog of the coupled vorticity-bond orientation modes discussed in Sec. III B. As q tends to zero, free disclinations now produce one viscous shear mode

$$\omega_t^-(q,\xi_\psi) \simeq -(\eta/mn_0)q^2 i \quad , \tag{6.33}$$

and a frequency which controls the relaxation of $\vec{v}_h$,

$$\omega_t^+(q,\xi_\psi) \approx -(\gamma_0/\epsilon_c)i \sim -\xi_\psi^{-2} i \quad . \tag{6.34}$$

Note that the coefficient of q^2 in (6.33) remains finite as $T \to T_i^+$, in contrast to the behavior of the viscosity near T_m. The frequency ω_t^+, on the other hand exhibits pronounced critical slowing down. It is interesting to note that (6.33) and (6.34) are what could be expected on the basis of dynamic scaling arguments[35] applied to this problem: Since K_A is finite at T_i^-, one expects the hydrodynamics sketched in Sec. III B to be qualitatively correct even at T_i^-. Hence, if dynamic scaling is to hold at all, frequencies must scale with a characteristic exponent

$$z_6 = 2 \quad . \tag{6.35}$$

Equations (6.33) and (6.34) are the only results consistent with this exponent and liquid hydrodynamics.

The transverse part of $\vec{v}_h$, which decouples from the remaining four variables, has the characteristic frequency

$$\omega_0(q,\xi_\psi) = -[(\gamma_0/\epsilon_c) + D_6 q^2]i \approx -(\gamma_0/\epsilon_c)i \sim -\xi_\psi^{-2} i \quad . \tag{6.36}$$

According to (6.29), this is also the relaxation rate for $S_{\text{free}}(\vec{r},t)$. We can think of this frequency as describing in a rough way the relaxation of fluctuations in the *amplitude* of the hexatic order parameter [i.e., in ψ_0, where $\psi = \psi_0 \exp(6i\theta)$], since these fluctuations are represented in the present model by the vortex cores in S_{free}.

The longitudinal modes decouple from the disclination dynamics in this approximation, and we recover the longitudinal eigenfrequencies quoted in Sec. III A. One would not expect longitudinal sound to couple in an important way to vorticity–bond-angle excitations, since it relaxes much more rapidly. Indeed, the situation seems rather analogous to first sound near the λ temperature in superfluid helium.[41] Because of mode coupling nonlinearities, neglected in the above analysis, compressional sound can, in fact, decay into vorticity and bond-orientation modes. One might expect a small anomaly in the damping due to these nonlinear effects.

E. Hexatic dynamics in a Lennard-Jones fluid

Our discussion of dynamics near the disclination unbinding transition has left open the question of whether the transverse hexatic frequencies just below T_i are purely diffusive or have instead a real part proportional to q^2. The answer to this question is nonuniversal, depending on hydrodynamic parameters not fixed by the theory. However, with slightly more information, obtained from experiment or computer simulations, it is possible to make a prediction. Frenkel and McTague[15] have studied a two-dimensional Lennard-Jones fluid, and found evidence for a hexatic phase bordered by low-temperature solid and high-temperature liquid phases. They examined, in particular, the relaxation of transverse momentum currents in the liquid and hexatic phases. It is possible to estimate the transverse hexatic frequencies just below T_i, from their measurements of the $\omega = 0$ transverse-momentum autocorrelation function.

To make contact with this simulation, we calculate the transverse-momentum autocorrelation function below T_i, by adding appropriate Langevin noise sources to the equations for the transverse hexatic modes. Since disclinations are bound, we neglect disclination currents, and use the linearized hydrodynamic equations discussed in Sec. III B. Upon defining

$$g_T(\vec{q},t) \equiv \vec{q} \times \vec{g}(\vec{q},t)/q \quad , \tag{6.37}$$

and

$$\nu = \eta/mn_0 \quad , \tag{6.38}$$

we have

$$\frac{\partial g_T(\vec{q},t)}{\partial t} = -\nu q^2 g_T(\vec{q},t) + \tfrac{1}{2} K_A i q^3 \theta(\vec{q},t) + \zeta(\vec{q},t) \quad , \tag{6.39a}$$

$$\frac{\partial \theta(\vec{q},t)}{\partial t} = -\kappa q^2 \theta(\vec{q},t) + \frac{1}{2mn_0} i q g_T(\vec{q},t) + \Upsilon(\vec{q},t) \quad , \tag{6.39b}$$

where the Gaussian noise sources $\zeta(\vec{q},t)$ and $\Upsilon(\vec{q},t)$ satisfy

$$\langle \zeta(\vec{q},t)\zeta(\vec{q}',t') \rangle = 2\eta k_B T q^2 \delta(\vec{q}+\vec{q}')\delta(t-t') \quad , \tag{6.40a}$$

$$\langle \Upsilon(\vec{q},t)\Upsilon(\vec{q}',t') \rangle = 2\Gamma_6 k_B T \delta(\vec{q}+\vec{q}')\delta(t-t') \quad . \tag{6.40b}$$

From these equations, one readily finds the transverse-momentum autocorrelation function,

$$G_T(q,\omega) \equiv \langle |g_T(\vec{q},\omega)|^2 \rangle / (k_B T 2mn_0) = \frac{\nu q^2(\omega^2 + \kappa^2 q^4) + (K_A/4mn_0)\kappa q^6}{|\Delta(q,\omega)|^2} \quad , \tag{6.41}$$

where

$$\Delta(q,\omega)=\omega^2+(\nu+\kappa)q^2i\omega-[\nu\kappa+(K_A/4mn_0)]q^4 \ . \tag{6.42}$$

There are poles in $G_T(q,\omega)$ at the characteristic hydrodynamic frequencies $\omega_t^{\pm}(q)$ discussed in Sec. III B. Fourier-transforming in time, one sees immediately that $G_T(q,t)$ is a weighted sum of *two* exponential decays, with characteristic times $\omega_t^{\pm}(q)$.

Upon defining an effective viscous parameter

$$\nu_{\rm eff}\equiv\lim_{q\to 0}[q^2G_T(q,\omega=0)]^{-1} \ , \tag{6.43}$$

it follows immediately from (6.41) that

$$\nu_{\rm eff}\equiv\eta_{\rm eff}/mn_0=\nu[1+(K_A/4\kappa\nu mn_0)] \ . \tag{6.44}$$

Remembering that $\nu=\eta/mn_0$, we see that this is the same effective viscosity that would be measured in the macroscopic "free boundary condition" experiment discussed in Appendix A.

This effective viscosity is enhanced over its value in the liquid, due to the coupling to the slowly relaxing bond-orientation field. Frenkel and McTague actually observe a shoulder in $\nu_{\rm eff}$ at T_i which can be understood in this way. Above T_i, where $\nu_{\rm eff}=\nu$, they find a viscosity which is roughly temperature independent,[15]

$$\nu\approx 1.5\sigma\sqrt{\epsilon/m} \ , \tag{6.45}$$

where σ, ϵ, and m are the length, energy, and mass parameters of the Lennard-Jones system. Since the dynamical theory of the previous subsection suggests that ν is nondivergent as $T\to T_i^+$, we assume that ν has roughly this same value below T_i. As observed in Ref. 15, $\nu_{\rm eff}$ increases by about 50% upon passing through T_i. From Fig. 3 of this reference, we estimate that

$$\nu_{\rm eff}\approx 2.3\sigma\sqrt{\epsilon/m} \tag{6.46}$$

just below T_i in the hexatic phase. According to Eq. (6.17), one further piece of information can be extracted from the value of the disclination unbinding temperature, $k_BT_i=0.57\epsilon$. One must have

$$K_A(T_i^-)=(72/\pi)k_BT_i=13.1\epsilon \ . \tag{6.47}$$

Substituting Eqs. (6.47), (6.46), and (6.45) into Eq. (6.44), together with the appropriate density ($n_0=0.8\sigma^{-2}$), we can solve for the only remaining hydrodynamic parameter just below T_i,

$$\kappa=5.1\sigma\sqrt{\epsilon/m} \ . \tag{6.48}$$

Substituting these results into the formulas compiled in Sec. III B, we find two purely diffusive transverse hydrodynamic frequencies,

$$\omega_t^+(q)=-4.1\sigma\sqrt{\epsilon/m}\,q^2i \ , \tag{6.49a}$$

$$\omega_t^-(q)=-2.5\sigma\sqrt{\epsilon/m}\,q^2i \ . \tag{6.49b}$$

The necessary inequality for diffusive modes (3.19) $(K_A/mn_0)<(\kappa-\nu)^2$ holds close to T_i because of the rather large value of κ. This is the product of a relaxation rate Γ_6 and K_A, which is bounded from below by $(72/\pi)k_BT$. This product will be rather large if Γ_6 and k_BT_i are of order unity in Lennard-Jones units. As T_m is approached from above, the analysis of Sec. V B shows that ν as well as K_A diverge like ξ_+^2, while κ remains finite. Therefore, close to T_m the inequality holds due to a large value of ν. Hence $\kappa-\nu$ must vanish for some temperature T_0, $T_m<T_0<T_i$, so that the transverse eigenfrequencies acquire a real part over some temperature interval within the hexatic phase. The imaginary part probably dominates at all temperatures, however. From calculations of $\nu_{\rm eff}$ only one cannot infer whether at some temperature T the hexatic modes are actually propagating or overdamped. Further information on the dynamic autocorrelation function $G_T(q,\omega)$ is needed.

From Eq. (6.44) we see that $\nu_{\rm eff}$ diverges like ξ_+^2 as $T\to T_m^+$. Frenkel and McTague[15] do in fact find a strong increase in $\nu_{\rm eff}$ near T_m. Finite size effects in a numerical simulation will, however, change the exponential increase of $\nu_{\rm eff}$ in an infinite system (6.36) to a rise in $\nu_{\rm eff}$ from its value in the hexatic phase to a very large value in the solid phase. (The value of $\nu_{\rm eff}$ should be infinite in the solid but is limited by finite-size effects in the numerical simulation).

ACKNOWLEDGMENTS

The authors are grateful for helpful conversations with N. Amer, D. Frenkel, P. C. Martin, J. McTague, and R. Morf. This work was supported in part by the National Science Foundation through the Harvard Materials Research Laboratory, and through Grant No. DMR 77-10210. One of the authors (A. Z.) was supported by a grant from the Deutsche Forschungsgemeinschaft, while another (D. R. N) was supported in part by a grant from the A. P. Sloan Foundation.

APPENDIX A: VISCOSITY IN THE HEXATIC PHASE

In this appendix, we examine the relation between the transport coefficients of the hexatic phase and the results of a conventional viscosity measurement applied to a film in the hexatic state. We shall see that the results depend on details of the experiment.[42]

For an idealized experiment let us consider a system which is infinite in the y direction, and confined

by walls (i.e., lines) at $x=0$ and $x=W$. We assume that the wall at $x=0$ is stationary, while the wall at $x=W$ is moving in the y direction at a velocity V_y. For a conventional fluid, in the limit where W is large compared to the atomic scale, and where V_y/W is small, compared to atomic relaxation rates, the steady state will have a momentum density g_y, which increases linearly with x, with

$$g_y=\begin{cases}0, & x=0\\ n_0 m V_y, & x=W.\end{cases} \tag{A1}$$

If the force per unit length on the walls is f, then the stress tensor is given by

$$\sigma_{xy}=\sigma_{yx}=f \ , \tag{A2}$$

and the liquid shear viscosity can be obtained from

$$\eta=\sigma_{xy}W/V_y \ . \tag{A3}$$

Boundary effects can be separated from the viscosity that one wishes to measure, by repeating the measurements for several values of W, and extrapolating appropriately to the limit of infinite W.

Let us now consider the results of such a measurement when the film is a liquid crystal, obeying the hydrodynamic equations (3.12)–(3.14). The relation for the stress tensor, which leads to (3.13), may be written as

$$\begin{aligned}\sigma_{ij}=&\tfrac{1}{2}K_A(\epsilon_{ik}\partial_k\partial_j\Theta+\epsilon_{jk}\partial_k\partial_i\Theta)\\ &+(\eta/mn_0)[\partial_i g_j+\partial_j g_i-(\vec{\nabla}\cdot\vec{g})\delta_{ij}]\\ &+(\zeta/mn_0)\delta_{ij}\vec{\nabla}\cdot\vec{g}-(B/n_0)\delta n \ .\end{aligned} \tag{A4}$$

In the present geometry, $g_x=\delta n=0$, and we may assume that all quantities are independent of y. Then

$$\sigma_{yx}=-\tfrac{1}{2}K_A\partial_x^2\Theta+(\eta/mn_0)\partial_x g_y \ . \tag{A5}$$

For a steady state, we assume $\partial g_y/\partial t=0$, and $\partial^2\Theta/\partial x\,\partial t=0$, whence, using (3.13) and (3.14):

$$\partial_x\sigma_{yx}=-\tfrac{1}{2}K_A\partial_x^3\Theta+(\eta/mn_0)\partial_x^2 g_y=0 \ , \tag{A6}$$

$$(1/2mn_0)\partial_x^2 g_y+\kappa\partial_x^3\Theta=0 \ . \tag{A7}$$

From these equations it follows that $\partial_x^3\Theta=\partial_x^2 g_y=0$, and hence from the boundary conditions (A1):

$$g_y(x)=mn_0V_y x/W \ . \tag{A8}$$

The value of $\partial_x^2\Theta$, and thence the stress tensor (A5) depends on the boundary condition for Θ.

If we assume "free boundary" conditions on Θ, which is to say $\partial_x\Theta=0$ at $x=0$ and $x=W$ then we find $\partial_x\Theta=\partial_x^2\Theta=0$, everywhere, and $\sigma_{yx}=\eta V_y/W$. The effective viscosity measured under these conditions is given by

$$\eta_{\rm eff}\equiv W\sigma_{yx}/V_y=\eta \ . \tag{A9}$$

Note that under these conditions, Eq. (3.14) becomes

$$\frac{\partial\Theta}{\partial t}=\frac{V_y}{2W} \ . \tag{A10}$$

Thus the bond orientations precess at a constant rate, everywhere in the sample.

A different situation occurs if we assume that the bond orientations are pinned at the walls, so that $\partial\Theta/\partial t=0$ for $x=0$ and $x=W$. Now a steady-state solution requires $\partial\Theta/\partial t=0$ everywhere, and hence, from (3.14),

$$\partial_x^2\Theta=-(1/2mn_0\kappa)\partial_x g_y \ . \tag{A11}$$

Under these conditions we find an effective viscosity

$$\eta_{\rm eff}=W\sigma_{yx}/V_y=\eta+\tfrac{1}{4}K_A/\kappa \ . \tag{A12}$$

This is identical to the quantity $\eta_{\rm eff}$ defined in terms of the momentum-density correlation function in Eq. (6.44).

As one approaches the temperature T_m from the hexatic side, the coefficient η and K_A are predicted to diverge as ξ_+^2, while κ remains finite. Thus, the two terms on the right-hand side of (A12) are found to have the same temperature dependence.

The viscosity of an isotropic fluid can also be obtained from the viscous penetration depth in an ac experiment. For example, if a wall at $x=0$ is made to oscillate at a frequency ω, and if the width W is sufficiently large, then the momentum density g will vary exponentially with x, as

$$g_y(x)\propto e^{-\alpha x} \ , \tag{A13}$$

$$\alpha=(\omega mn_0/\eta)^{1/2} \ . \tag{A14}$$

In the hexatic phase, when Eq. (3.20) applies, there will be two exponential decaying modes at the given frequency ω. The inverse decay lengths are given by

$$\alpha_\pm=(2\omega/D_\pm)^{1/2} \ , \tag{A15}$$

where $D_\pm$ are given in Eq. (3.21). At large distances from the wall, only the slower exponential is important, corresponding to the choice D_+ in (A15). Close to the solidification transition ($T\to T_m^+$) the value of D_+ is equal to $2\eta/mn_0$, so that α_+ is then related to η by an expression identical to that applicable to the liquid phase, Eq. (A14).

APPENDIX B: BURGERS-VECTOR CURRENT WITH $D_\parallel\neq D_\perp$

In this appendix we evaluate the Burgers-vector current $\langle J_i^n\rangle$ for the general case $D_\parallel\neq D_\perp$. Using the conservation law for the total Burgers-vector density

(4.28), we can write (5.7) as

$$\langle J_i^n \rangle = -C_{ikl}^n(\sigma_{kl}+\bar{p}\delta_{kl}) - iD_{il}^{nk}(k_l k_j/\omega)\langle J_j^k \rangle \ . \tag{B1}$$

To eliminate $k_j\langle J_j^k\rangle$ in terms of $(\sigma_{kl}+\bar{p}\delta_{kl})$ we multiply both sides of (B1) by k_i

$$[G_T^{-1}P_{nl}^T(\vec{k})+G_L^{-1}P_{nl}^L(\vec{k})]k_j\langle J_j^l\rangle = -k_i C_{ikl}^n(\sigma_{kl}+\bar{p}\delta_{kl}) \ , \tag{B2}$$

where $P_{nl}^{T,L}(\vec{k})$ are transverse and longitudinal projectors

$$P_{nl}^T(\vec{k}) = \delta_{nl} - k_n k_l/k^2 \ , \quad P_{nl}^L(\vec{k}) = k_n k_l/k^2 \ , \tag{B3}$$

and

$$G_T^{-1} = 1 + i\frac{k^2}{\omega}\frac{D_{\parallel}+3D_{\perp}}{4} \equiv \alpha \ ,$$
$$G_L^{-1} = 1 + i\frac{k^2}{\omega}\frac{3D_{\parallel}+D_{\perp}}{4} \equiv \beta \ . \tag{B4}$$

The matrix $[\alpha P_{nl}^T(k)+\beta P_{nl}^L(k)]$ is easily inverted, to yield $k_j\langle J_j^l\rangle$ in terms of $\sigma_{kl}+\bar{p}\delta_{kl}$. Equation (B1) can then be rewritten

$$\langle J_i^n\rangle = -C_{ikl}^n(\sigma_{kl}+\bar{p}\delta_{kl}) + \frac{i}{\omega}D_{it}^{nl}k_t\left[\frac{1}{\alpha}P_{lm}^T(\vec{k})+\frac{1}{\beta}P_{lm}^L(\vec{k})\right]k_j C_{jks}^m(\sigma_{ks}+\bar{p}\delta_{ks}) \ . \tag{B5}$$

For $\vec{k}$ in the x direction, the four independent components of $\langle J_i^n\rangle$ are given by

$$\langle J_x^x\rangle = \frac{n_f a_0}{k_B T}\frac{D_{\parallel}+D_{\perp}}{2}\sigma_{xy}G_L \ , \tag{B6}$$

$$\langle J_y^y\rangle = -\langle J_x^x\rangle[1+(ik^2/\omega)D_{\parallel}] \ , \tag{B7}$$

$$\langle J_x^y\rangle = -\frac{n_f a_0}{k_B T}G_T\left[\frac{D_{\parallel}+D_{\perp}}{2}(\sigma_{xx}+\bar{p}) - \frac{(D_{\parallel}+3D_{\perp})}{4}(\sigma_{ii}+2\bar{p})\right] \ , \tag{B8}$$

$$\langle J_y^x\rangle = \frac{n_f a_0}{k_B T}G_T\left[\frac{D_{\parallel}-D_{\perp}}{4}(\sigma_{ii}+2\bar{p}) - \frac{D_{\parallel}+D_{\perp}}{2}(\sigma_{xx}+\bar{p})\left(1+\frac{ik^2}{\omega}D_{\parallel}\right)\right] \ . \tag{B9}$$

APPENDIX C: TRANSPORT COEFFICIENTS AND TRANSVERSE MODES NEAR T_m

We present here the method used to obtain the transport coefficients of the hexatic phase and the transverse hydrodynamic modes, near T_m, from the equations of motion of the dislocation plasma, developed in Sec. V, Eqs. (5.11)–(5.14). Actually, we shall use rather than (5.14), the constitutive relations developed in Appendix B, for the more general case where $D_{\parallel} \neq D_{\perp}$. The analysis of the longitudinal modes can be carried out in a similar fashion.

Before we analyze the equations of motion at finite $\vec{k}$ and ω, let us calculate the viscosity η in the hexatic phase by analyzing the dc experiment described in Appendix A, in which the substance is bounded by a stationary wall at $x=0$ and a moving wall at $x=W$, with free boundary conditions on the orientation angle Θ. In this experiment, we reach a steady state, with σ_{yx} a constant, and $g_y = g'x$, where $g' = n_0 m V_y/W$. We expect, by symmetry that the Burgers-vector currents $\langle J_x^x\rangle$ and $\langle J_y^y\rangle$ will be nonzero, but independent of position, while

$$\langle \mathfrak{B}_x\rangle = \langle \mathfrak{B}_y\rangle = \langle J_x^y\rangle = \langle J_x^y\rangle = 0 \ .$$

From Eqs. (5.11) and (5.12), we see that in this geometry

$$\frac{1}{n_0 m}\frac{\partial g_y}{\partial x} + a_0(\langle J_y^y\rangle - \langle J_x^x\rangle) = \frac{\partial}{\partial t}(w_{yx}+w_{xy}) \ . \tag{C1}$$

Since $(w_{yx}+w_{xy}) = \sigma_{yx}/\mu_0$, the right-hand side of (C1) must vanish in the steady state. From Eqs. (B1) and (5.8a) we find

$$\langle J_x^x\rangle = -\langle J_y^y\rangle = \nu_0 a_0^{-1}\sigma_{xy} \ , \tag{C2}$$

where

$$\nu_0 \equiv \frac{n_f a_0^2}{k_B T}\frac{D_{\parallel}+D_{\perp}}{2} \ . \tag{C3}$$

Note that Eqs. (C2) and (C3) reduce to Eqs. (5.14a)–(5.14c) in the case $D_{\parallel}=D_{\perp}$. Using Eqs. (A9), we see immediately that

$$\eta = \frac{\sigma_{xy}n_0 m}{g'} = \frac{1}{2\nu_0} \ , \tag{C4}$$

which is the result quoted in (5.19).

If instead of free boundary conditions we had assumed that dislocations could not be created or destroyed at the boundary, we would have had to introduce a nonvanishing gradient of the Burgers-vector density $\langle \mathfrak{B}_x \rangle$, so that the current $\langle J_x^x \rangle$ would vanish. The analysis in that case would lead to a result for the effective viscosity (A12).

Let us now consider the dynamic equations (5.11)–(5.13), (A6), and (A7), at finite k and ω. For simplicity we shall choose units where $n_0 m = a_0 = 1$. After some manipulation, we can obtain three coupled equations for the quantities σ_{xy}, g_y, and $\langle \mathfrak{B}_x \rangle$, which we write in matrix form as

$$+i\omega \begin{pmatrix} \sigma_{xy} \\ g_y \\ \langle \mathfrak{B}_x \rangle \end{pmatrix} = \begin{pmatrix} 2\nu_0\mu_0 & -ik\mu_0 & -\frac{1}{2}ik(D_\parallel + D_\perp)\mu_0 \\ -ik & 0 & 0 \\ ik\nu_0 & 0 & (\frac{3}{4}D_\parallel + \frac{1}{4}D_\perp)k^2 \end{pmatrix} \begin{pmatrix} \sigma_{xy} \\ g_y \\ \langle \mathfrak{B}_x \rangle \end{pmatrix} . \tag{C5}$$

The eigenvalues of this equation are the roots of the cubic equation

$$(i\omega)^3 - (i\omega)^2(\tilde{D}k^2 + 2\nu_0\mu_0) + (i\omega)(\nu_0\mu_0 D_\parallel k^2 + \mu_0 k^2) - \mu_0 \tilde{D} k^4 = 0 , \tag{C6}$$

where

$$\tilde{D} \equiv \tfrac{3}{4}D_\parallel + \tfrac{1}{4}D_\perp . \tag{C7}$$

In the limit $k \to 0$, the eigenvalues become

$$\omega = -2i\nu_0\mu_0 , \tag{C8}$$

$$\omega = -\tfrac{1}{2}ik^2 D_\pm \tag{C9}$$

with

$$\tfrac{1}{2}D_\pm = \frac{\mu_0 + \mu_0\nu_0 D_\parallel \pm [(\mu_0 + \mu_0\nu_0 D_\parallel)^2 - 8\mu_0^2\nu_0\tilde{D}]^{1/2}}{4\mu_0\nu_0} . \tag{C10}$$

Close to T_m, where ν_0 is small, we find

$$\tfrac{1}{2}D_+ = 1/(2\nu_0) , \tag{C11}$$

$$\tfrac{1}{2}D_- = \tilde{D} . \tag{C12}$$

For frequencies of order k^2, in the hydrodynamic limit $k \to 0$, the three equations (C5) can be reduced to two. From the first row of (C5), we see that in this limit,

$$2\nu_0\sigma = ikg + \tfrac{1}{2}ik(D_\parallel + D_\perp)\langle \mathfrak{B} \rangle , \tag{C13}$$

where we have suppressed the Cartesian indices on the variables. We can then use this to eliminate σ_{xy} from the second and third rows of (C5) giving

$$i\omega g = \frac{k^2}{2\nu_0}g + \frac{k^2(D_\parallel + D_\perp)}{4\nu_0}\langle \mathfrak{B} \rangle , \tag{C14}$$

$$i\omega\langle \mathfrak{B} \rangle = -\tfrac{1}{2}k^2 g + \tfrac{1}{2}D_\parallel k^2 \langle \mathfrak{B} \rangle . \tag{C15}$$

In order to compare directly with the hydrodynamic equations for the hexatic state, we would like to eliminate $\langle \mathfrak{B} \rangle$ in favor of the variable $\theta = \frac{1}{2}(w_{xy} - w_{yx})$. Using Eqs. (5.11)–(5.13), (B6), and (B7), one finds that

$$2\omega\theta = kD_\parallel \langle \mathfrak{B} \rangle - kg . \tag{C16}$$

After some algebra, one can obtain from (C14)–(C16) two equations of the hydrodynamic form,

$$-i\omega g = \tfrac{1}{2}iK_A k^3\theta - \eta k^2 g , \tag{C17}$$

$$-i\omega\theta = \tfrac{1}{2}ikg - \kappa k^2\theta , \tag{C18}$$

where η is given by (C4) and K_A and κ are given by

$$\kappa = \tfrac{1}{2}D_\parallel , \tag{C19}$$

$$K_A = k_B T/n_f a_0^2 . \tag{C20}$$

[1] J. M. Kosterlitz and D. J. Thouless, J. Phys. C 6, 1181 (1973).

[2] J. M. Kosterlitz and D. J. Thouless, Prog. Low Temp. Phys. 7B, 371 (1978).

[3] See, e.g., W. Shockley, in *L'Etat Solide*, Proceedings of the Neuvième Conseil de Physique, edited by R. Stoops (Institut International de Physique Solvay, Brussels, 1952); D. Kuhlmann-Wilsdorf, Phys. Rev. 140, A1599 (1965); and T. Ninomiya, J. Phys. Soc. Jpn. 44, 263, 269 (1978).

[4] D. R. Nelson, Phys. Rev. B 18, 2318 (1978).

[5] B. I. Halperin and D. R. Nelson, Phys. Rev. Lett. 41, 121, 519(E) (1978); D. R. Nelson and B. I. Halperin, Phys. Rev. B 19, 2457 (1979).

[6] A. P. Young, Phys. Rev. B 19, 1855 (1979).

[7] K. G. Wilson and J. Kogut, Phys. Rep. 12C, 77 (1977).

[8] See, e.g., J. G. Dash, *Films on Solid Surfaces* (Academic, New York, 1975).

[9] C. C. Grimes and G. Adams, Phys. Rev. Lett. 42, 795 (1979); see also D. S. Fisher, B. I. Halperin, and P. Platzman, Phys. Rev. Lett. 42, 7 (1979).

[10] C. Y. Young, R. Pindak, N. A. Clark, and R. B. Meyer, Phys. Rev. Lett. 40, 773 (1978).

[11] C. Rosenblatt, R. Pindak, N. A. Clark, and R. B. Meyer, Phys. Rev. Lett. 42, 1220 (1979).

[12] R. J. Birgeneau and J. D. Litster, J. Phys. (Paris) Lett. 39, L399 (1978).

[13]See, e.g., H. Burecki and N. M. Amer, J. Phys. (Paris) Colloq. 40, C3-433 (1979), and references therein.
[14]See, e.g., M. Joly, Kolloid Z. 63, 26 (1939), and Ref. 13.
[15]D. Frenkel and J. D. McTague, Phys. Rev. Lett. 42, 1632 (1979); for earlier work emphasizing the importance of dislocations, see R. M. J. Cotterill and L. B. Pederson, Solid State Commun. 10, 439 (1972). The existence of a hexatic phase in the 2D Lennard-Jones system is quite controversial, however. See F. van Swol, L. V. Woodcock, and J. N. Cape (unpublished); F. F. Abraham, Phys. Rev. Lett. 44, 463 (1980); and F. Toxvaerd, Phys. Rev. Lett. 44, 1002 (1980). See also Proceedings of the International Conference on Ordering in Two-Dimensions, Lake Geneva, Wisc., May 1980 (North-Holland, Amsterdam, in press.)
[16]R. Morf, Phys. Rev. Lett. 43, 931 (1979).
[17]See, e.g., D. Forster, *Hydrodynamic Fluctuations, Broken Symmetry, and Correlation Functions* (Benjamin, Reading, Mass., 1975).
[18]P. G. de Gennes, *The Physics of Liquid Crystals* (Oxford University Press, London, 1974), and references therein.
[19]P. C. Martin, O. Parodi, and P. S. Pershan, Phys. Rev. A 6, 2401 (1972).
[20]L. D. Landau and E. M. Lifshitz, *Theory of Elasticity* (Pergamon, New York, 1970).
[21]See, e.g., Y. Pomeau and P. Résibois, Phys. Rep. 19C, 64 (1975), and references therein; see also, D. Forster, D. R. Nelson, and M. J. Stephen, Phys. Rev. A 16, 732 (1977).
[22]A. Zippelius, Phys. Rev. A (in press).
[23]P. C. Hohenberg and B. I. Halperin, Rev. Mod. Phys. 49, 435 (1977).
[24]F. R. N. Nabarro, *Theory of Dislocations* (Clarendon, New York, 1967).
[25]J. S. Langer and J. D. Reppy, Prog. Low Temp. Phys. 6, 1 (1970).
[26]V. Ambegaokar, B. I. Halperin, D. R. Nelson, and E. D. Siggia, Phys. Rev. Lett. 40, 783 (1978); Phys. Rev. B 21, 1806 (1980).
[27]D. J. Bishop and J. D. Reppy, Phys. Rev. Lett. 40, 1727 (1978).
[28]L. Landau and E. M. Lifshitz, *Statistical Physics* (Pergamon, New York, 1959).
[29]F. Jähnig and H. Schmidt, Ann. Phys. (N.Y.) 71, 129 (1972).
[30]L. Landau and E. M. Lifshitz, *Fluid Mechanics* (Pergamon, New York, 1959).
[31]See chapter 11 of Ref. 17.
[32]M. J. Stephen, Phys. Rev. A 2, 1558 (1970); D. Forster, T. C. Lubensky, P. C. Martin, J. Swift, and P. S. Pershan, Phys. Rev. Lett. 26, 1016 (1971); see also Refs. 19 and 29.
[33]M. Peach and J. S. Koehler, Phys. Rev. 80, 436 (1950).
[34]D. S. Fisher, B. I. Halperin, and R. H. Morf, Phys. Rev. B 20, 4692 (1979).
[35]R. A. Ferrell, N. Menyhard, H. Schmidt, F. Schwabl, and P. Szépfalusy, Phys. Rev. Lett. 18, 891 (1967); B. I. Halperin and P. C. Hohenberg, Phys. Rev. 177, 952 (1969). For a discussion of the breakdown of dynamic scaling at the two-dimensional superfluid transition, see P. C. Hohenberg, B. I. Halperin, and D. R. Nelson, Phys. Rev. B (in press).
[36]V. Ambegaokar and S. Teitel, Phys. Rev. B 19, 1667 (1979).
[37]J. M. Kosterlitz, J. Phys. C 7, 1046 (1974).
[38]H. Lamb, *Hydrodynamics*, 6th ed. (Dover, New York, 1932).
[39]This form for $J_{6,\text{free}}$ with its proportionality to the disclination force and the gradient of $S(\vec{r},t)$, is very similar, e.g., to the corresponding expression for electrons and holes in semiconductors. See N. W. Ashcroft and N. D. Mermin, *Solid State Physics* (Holt, Rinehart, and Winston, New York, 1976), Chap. 29.
[40]J. D. Jackson, *Classical Electrodynamics* (Wiley, New York, 1967).
[41]See, e.g., P. C. Hohenberg, in *Proceedings of the Enrico Fermi School of Physics, Course 51, Critical Phenomena*, edited by M. S. Green (Academic, New York, 1971).
[42]See for example Ref. 18, Chap. 5.